Discrete Comput Geom 6:225-262 (1991)

Discrete & Computational
Geometry

On the Global Structure of Crystalline Surfaces*

Jean E. Taylor

Mathematics Department, Rutgers University, New Brunswick, NJ 08903, USA

Abstract. We bound the number of plane segments in a crystalline minimal surface S in terms of its Euler characteristic, the number of line segments in its boundary, and a factor determined by the Wulff shape W of its surface energy function. A major technique in the proofs is to quantize the Gauss map of S based on the Gauss map of W. One thereby bounds the number of positive-curvature corners and the interior complexity of S.

1. Introduction

Let Φ, the surface energy per unit surface area, be a real-valued function defined on the unit sphere S^2. By the *surface energy* of a two-dimensional oriented surface S in R^3 we mean the integral

$$\Phi(S) \equiv \int_{x \in S} \Phi(\nu_S(x))\, dx,$$

when this is defined; here $\nu_S(x)$ denotes the unit oriented normal to S at $x \in S$ (which should be defined for almost all $x \in S$) and dx denotes integration with respect to two-dimensional surface measure. When Φ is a constant function, as in the case for an interface between liquids, this integral is proportional to the area of S. In this paper we consider the opposite extreme in which the Wulff shape W of Φ is a polyhedron instead of a sphere, and in which the surfaces S are polyhedral surfaces with boundary. (The Wulff shape is the equilibrium shape of a single isolated region; see Section 2 for definitions and Fig. 1 for the Wulff shape which we use for the examples of Section 6.)

*The support of the National Science Foundation and the Air Force Office of Scientific Research and the hospitality of Stanford University, where this paper was extensively rewritten, are gratefully acknowledged.

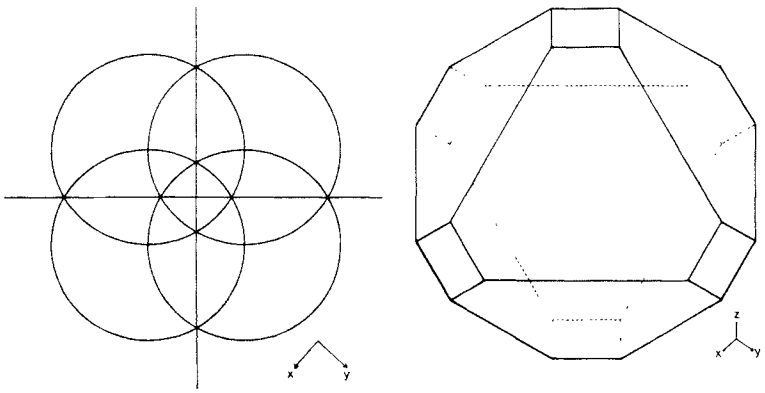

(a) (b)

Fig. 1. An n-diagram (see Section 2) in stereographic projection, and a Wulff shape with that n-diagram. Figures 7–12 assume that Φ is such that its Wulff shape has this n-diagram.

Suppose that S as above satisfies the following three properties (plane segments are defined later in this section and edges are defined in Section 4):

(S1) S is composed of a finite number of plane segments with polygonal boundaries (these plane segments certainly need not be convex),
(S2) S is a continuous submanifold of R^3 with boundary B, and
(S3) no polyhedral deformation of S within some neighborhood of any (closed) interior edge which fixes B can either decrease the surface energy of S or maintain the same energy and increase the volume of any solid it partially bounds.

Then a special case of the main result of this paper is that if the boundary B is in the kind of general position defined below, then the number of plane segments of S is bounded *a priori* in terms of the structure of W, the Euler characteristic of S (which is determined by the number of connected components and handles of S and the number of cycles in its boundary B), and the number of line segments in the boundary B. That is, in this case and in the other cases treated in this paper, how combinatorially complicated S can be in its middle is determined by its structure out near its boundary and its Euler characteristic and by which integrand measures its surface energy.

The idea of the proof of the bound is to show that the Gauss map (and hence Gauss curvature) of S comes in the "quanta" given by the generalized Gauss maps of the corners of W, and that positive Gauss curvature comes in isolated individual quanta. The Euler characteristic together with the boundary curvature gives us the net curvature (Gauss–Bonnet, reproved in Lemma 3 for completeness), so the quantization gives the bound if there is control over the amount of positive curvature. We obtain this bound by counting in two ways how much S bends up and down. Many difficulties arise due to the nongeneric positions of plane segments and to their behavior at the boundary, but if for the moment we ignore all

this and define quantities very loosely, the basic structure of the proof of this bound can be explained as follows.

All edges E of the surface are taken to be oriented (and so interior edges are counted twice). Additionally, each interior edge is of either *regular* or *inverse* type, depending on whether the oriented normals to its adjacent plane segments point "away from" or "toward" each other, and edges in the boundary are labeled by a convention described in Section 4. A basic parameter is the "label switch" n defined on edges by $n(E) = 1$ if the type of E differs from the type of the edge following E in the boundary of the (unique) plane segment E partially bounds, and define $n(E) = 0$ otherwise (except in special cases; see Section 4). For (standard) positive-curvature corners, $n(E) = 0$ for each edge coming into the corner, and so the sum over these incoming edges of $1 - n(E)/2$ is at least three, since there are at least three edges coming into each interior corner. For nonpositive-curvature interior corners, this sum is at least two, since it must be an integer and each edge (except for those special cases) contributes 1 or $\frac{1}{2}$ to the sum. Thus the number of positive-curvature corners plus twice the number of *all* corners is dominated by the sum over all oriented edges of $1 - n(E)/2$, up to difficulties we are ignoring. The sum of $n(E)$ over all oriented edges can equally well be regarded as the sum over all plane segments of the sum around each plane segment of $n(E)$. The sum around a plane segment of $n(E)$ (i.e., the number of times the surrounding planes change from bending up to bending down or vice versa) is shown in Proposition 5 to be at least four, under the hypotheses of this paper; note that this is analogous to area-minimizing surfaces being locally saddle-shaped. Therefore, except for boundary terms and other complications we ignore here, the number of positive-curvature corners is bounded above by the number of oriented edges, less twice the number of plane segments, less twice the number of corners — that is, by $-2\chi(S)$ (Propositions 4 and 6).

The phenomenon of curvature quantization is, as far as I know, a new mathematical device. Certainly it has been known for a long time (probably Gauss knew it!) that a generalized unit normal (Gauss) map and thus a Gauss curvature can be assigned to corners in polyhedral embedded surfaces, but here we have a fixed subdivision of the unit sphere induced by W and the generalized Gauss map of the surfaces under consideration is always a sum of these particular regions (or, in case more than three faces meet at some vertex of W, some triangulations of these regions using the same vertices) as was shown in [T2]. This is crucial to much of the paper.

Those who are combinatorially minded may also be intrigued both by the technique for counting positive-curvature corners as well as by the general combinatorial structure of these surfaces. Those interested in the shapes of physical interfaces where at least one of the regions is crystalline, including shapes which are quite topologically complex interfaces between interlocking regions as in Fig. 12, should find the results and their method of proof relevant.

Specifically, let S be an oriented finite abstract two-dimensional simplicial complex which is a PL-manifold with polygonal boundary B, together with an immersion of S in R^3 which is locally a continuous embedding, affine on each simplex. If we require S to be embedded in R^3, as a physical surface of a crystal

would be, then we can identify S with its embedding and not be concerned about the abstract manifold; the only harm in doing so is a loss of generality. (For example, the immersion of S could be derived from an integral currrent with multiplicity greater than one on various subsets.) We sometimes in fact drop the words "image of" and identify S with its immersion as if it were an embedding just for simplicity of language. By a **line segment of** B we mean a connected part of the boundary of S whose immersed image is a straight line segment in R^3 and which is maximal for this property. A **corner of** B is a common endpoint of two line segments of B. N_B is the number of line segments of B (and thus the number of corners of B).

By a **plane segment** P of S we mean a closed oriented subset of S (the union of finitely many closed triangles) such that its interior is connected, each triangle is embedded by the immersion in the same plane with the same orientation, and it is maximal in S with respect to these properties. Thus adjacent plane segments in S have different orienting normal vectors in the immersion. The immersion of a plane segment of S need not be convex. Neither need it be topologically a disk; it can have holes, and it can have one or more vertices on its boundary which are endpoints of four or more edges of its boundary, so that a small enough neighborhood of such a vertex intersected with the interior of P has more than one connected component. We use the terminology "plane segment" rather than "face" to emphasize the conditions that a plane segment must meet, and also to encompass the case where S is not embedded (even plane segments need not be embedded!) but is an abstract simplicial complex with many simplices per plane segment. An **interior corner** of S is a point of S which is in three or more plane segments of S and is not in B.

We define below surface properties H1–H3 which will always be required in this paper and possible other properties HZ and HB and prove that *any such S in R^3 which satisfies hypotheses S1, H1–H3, and either HZ or HB, has no more interior corners than*

$$(1 + A/a + \pi/a)(N_B - 2\chi(S)),$$

where N_B is the number of line segments in the boundary B of S, $\chi(S)$ is the Euler characteristic of S, and a (resp. A) is the area of the smallest (resp. largest) tie region or subregion of the n-diagram of W (defined in Section 2; these are the "quanta" referred to above). A much better bound can be given using more information about the boundary and the structure of S along the boundary; this bound is stated in Theorem 7, along with similar bounds on the number of plane segments and the relevant bounds if neither HZ nor HB holds.

In order to state hypotheses H2 and H3, we need to define the notion of convex and concave corners. At any interior corner p, the embedded image of a neighborhood S_p of p in S divides a small ball centered at the image of p into two pieces U_1 and U_2; let U_1 be the piece "behind" S, so that the embedding of S_p is part of the oriented boundary of U_1. If U_1 (resp. U_2) is convex, we say S has a convex (resp. concave) corner at p. (Normally, most corners of S are neither convex nor concave but "saddle-shaped".)

The hypotheses listed above are as follows:

H1. The images of the neighborhoods S_p of the interior corners p of S under the immersion gives configurations of the types in the catalog in [T2], and the images of the neighborhoods of corners of S on the boundary B gives configurations having Properties 1 and 2 of Section 4 of [T2] (see Section 3 below for a summary of the results of [T2]). In particular, the image of each plane segment of S lies in a plane parallel to a face of W (with the same orientation), and the embedded image of a sufficiently small neighborhood of each point of S is a Φ-minimizing surface in R^3 relative to its boundary.

H2. There are no concave interior corners in S, and if two adjacent plane segments in S have the property that the faces of W which are parallel to them touch only at a corner of W, then that edge of S is of *regular* type (see Section 3 below).

H3. If a plane segment P of S has three successive interior edges all of the same type (*regular* or *inverse*), and if P is convex at each of the two intervening corners, then the directions of P and the three plane segments adjacent to it along those edges are contained in the set of directions of faces meeting at a single vertex of W. In particular, if all corners of W are trivalent, there is no edge of S with interior convex corners at each end.

HZ. B is composed of line segments parallel to edges of W, and W is a generalized zonohedron: that is, each face of W has an even number of edges, and each pair of opposite edges on each face is parallel. (This was actually the original definition of the word zonohedron by the crystallographer Fedorov [F], but Coxeter [C1], [C2] has used a more restrictive definition which has by now become standard. See [T3] for more information concerning zonohedra.)

HB. The boundary is in a "general position" relative to the surface S, as defined by the criterion that each line segment of the boundary is contained in a single plane segment of S.

Assuming HZ and S1 hold and S is embedded, then H1–H3 are implied by properties S2 and S3. To see this, note first (as was shown in [T1]) that if S satisfies S1–S3, then all directions for plane segments in S except the normals of W are excluded by barrier arguments using tangent cones to corners of W, which are volume-maximising among Φ-minimizing surfaces with the same boundary, or tangent cones to edges of W or its central inversion, which are uniquely Φ-minimizing. (In the proof of this implication for Φ-minimizing integral currents in [T1], there is a gap, in that there is an implicit hypothesis of local finite connectivity which is not known to be satisfied in general but which is assumed here via S1 or H1.) Concave corners are prevented by use of the former type of barrier, and two convex corners which correspond to different corners of the Wulff shape at the ends of one edge are prevented by the use of barriers of the latter type. The proof that a

violation of the more general statement of H3 would lead to a violation of minimization of surface energy follows from that of Property 2 in Section 4 of [T2]: a trapezoid subset of P, with one of the parallel edges being the intersection with the middle plane segment and the two adjacent edges being parts of the intersections with the outer two plane segments, is cut out and translated a short distance in height; it is patched back into S by adding small triangles at the corners, cutting thin strips from the three neighboring planes, extending the trapezoid along its two nonparallel edges, and adding a thin trapezoid with its direction v being that of the middle plane segment adjacent to P. The proof that this decreases energy when H3 is violated is precisely that of [T2].

Hypotheses H1–H3 are better than hypotheses S2 and S3 in several respects: H1–H3 are somewhat more general, H1–H3 are the conditions actually used in the proof in this paper; and checking that H1–H3 hold clearly involves checking only a finite number of specific conditions (as opposed to "all deformations").

If HZ does not hold, then S1–S3 still limit the number of plane directions that can occur; here, however, plane segments containing a line segment of B might have certain non-W directions (see [T1]). The presence of such "extra" directions for plane segments destroys the quantization of Gauss maps described above and thus the key step in the proof of the theorem; it also affects Proposition 5(b). Thus one either has to include the number of interior corners of such non-W plane segments as part of the bound, or, in what amounts to the same thing, to exclude plane segments with "extra" directions by using a new surface S' with boundary B' which lies in S but cuts off those planes with bad directions. We cover both approaches by simply requiring all normals of plane segments of S to be contained in the set of normals to W; a further justification for this is to think of S as being a part of a larger overall surface, so where we put the boundary B is rather arbitrary anyway.

Volume maximization among surfaces of the same energy (or its implication as expressed in H2) is assumed because without some such assumption there can be no bound as in the theorem; see Fig. 2(a). It would, however, be equivalent to use volume minimization, which would mean interchanging the words convex and concave in H2 and H3 and replacing *regular* by *inverse*. Similarly, without H3 there can be no bound, since we could then put arbitrarily many small mesas in the

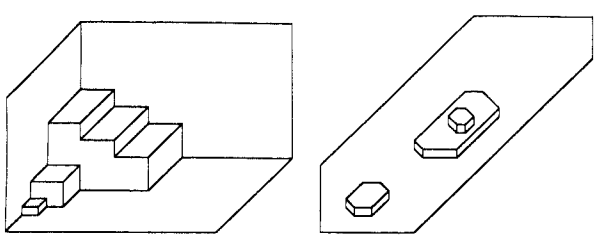

Fig. 2. Examples of surfaces for which there can be no *a priori* bound. Example (a) does not satisfy H2; example (b) does not satisfy H3.

middle of any plane segment, as in Fig. 2(b). Tents could also be constructed if we allowed non-Φ-minimizing convex corners; thus that part of the Φ-minimization hypothesis is required.

A reason to use HZ is that the bounds then do not depend on knowing the structure of S near B; it is thus better suited to the classical problem of finding a Φ-minimizing surface with a prescribed boundary. For this problem, however, the hypothesis that S be composed of a finite number of plane segments is major; general existence theorems only yield varifold or perhaps integral current solutions. We can speculate that it might be possible to bound the Euler characteristic of S by some function of N_B, and that such a bound would both address this issue of finiteness and provide an absolute upper bound to the number of plane segments of S independent of the Euler characteristic of S. But as things now stand, this paper establishes the curious result that **if** a volume-maximizing Φ-minimizing surface is composed of a finite number of plane segments and if the surface is locally embedded, then there is an *a priori* upper bound to the number of plane segments.

Hypotheses S1, H1, and H2 are not unreasonable from a physical point of view, since volume maximization among Φ-minimizing surfaces might well hold for an interface between two phases which has resulted from the slow growth of one phase into the other. But H3 (which is a consequence of Φ-minimization in the neighborhood of an edge, not a point, of S) may be a problem, since it is nonlocal. In particular, an interface may well not "see" that it can decrease surface free energy by retreating along a whole edge. Also, the system might be minimizing a free energy which includes more than surface free energy, or one that includes a volume constraint, or one which involves some other constraint. This configuration of two adjacent convex corners might therefore be minimizing for this other problem, as it is in the case of W itself. Even S1 and the requirement of only W-directions may fail to hold in these other problems, as it can for instance in the problem of the shape of a crystal under gravity [ATZ], [T5] or the shape of a surface near a grain boundary groove in the presence of a temperature gradient [VCMS].

The author has an algorithm for constructing surfaces having a prescribed boundary B and satisfying S1, S2, and H1–H3, and further for extracting one that is globally minimizing within this class, provided HZ holds and B is an extreme simple closed curve [T4]. This scheme has been implemented computationally; a sample result is shown in Fig. 3.

Six examples of surfaces and the way the various estimates of the paper apply to them are given in the last section. They should be consulted initially as examples of the types of surfaces which are considered in this paper, in Section 4 for examples of the definitions, and at the end as examples in connection with the more precise bounds of the main theorem and its preceding propositions.

This paper differs from earlier drafts primarily in that it handles arbitrary polyhedral Wulff shapes W, in particular those with nontrivalent corners and/or those that are not generalized zonohedra; it also keeps track of sources of inequality so that results can be explicitly stated for the case where neither HB nor HZ holds, and so that cases in which the bounds are exact can be identified.

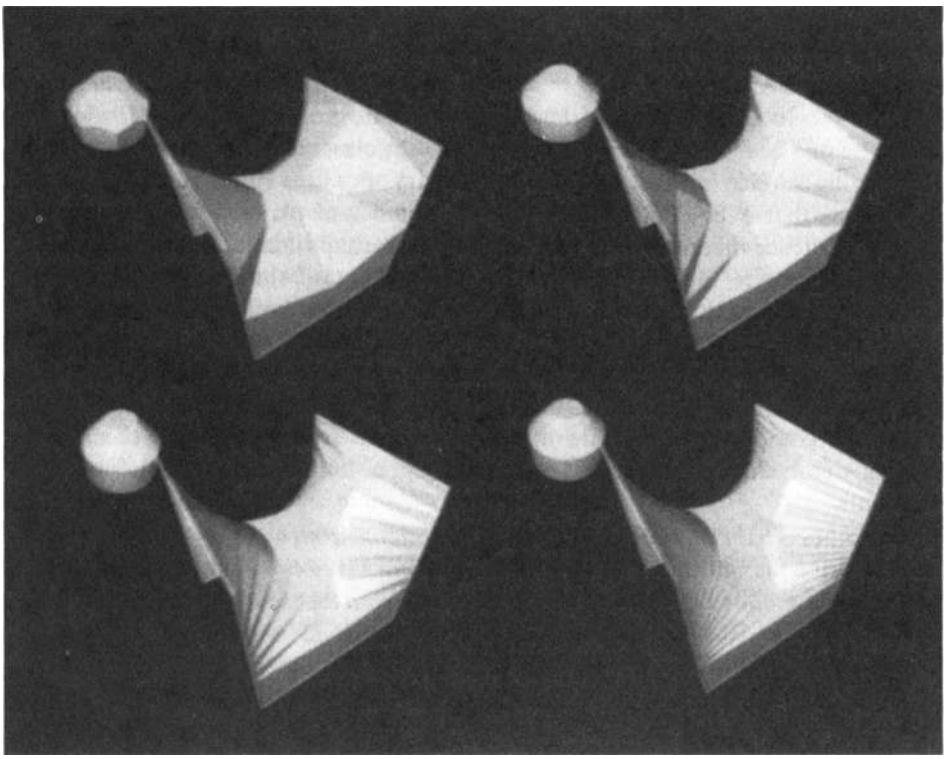

Fig. 3. Examples of the output of a program to compute Φ-minimal surfaces, consisting of surfaces on a boundary together with the convex bodies which are the Wulff shapes for the different Φ's.

2. W and Its n-Diagram

As in the introduction, let

$$\Phi: S^2 \to R$$

be given; Φ can be any function so that its Wulff shape

$$W \equiv \{x \in R^3 : x \cdot v \leq \Phi(v), \forall v \in S^2\}$$

is a region of positive (nonzero and noninfinite) volume. W is the analog of the unit sphere for the surface free energy function which is constantly 1; that is, W is the shape having a given volume for which the total surface free energy (as defined in Section 1) is the minimum possible value (see, for example, [T1] or better, [B1]). For the rest of this paper we assume that W is a polyhedron. We make no further assumptions on W or Φ in general; as part of the optional hypothesis HZ, we assume that W is a generalized zonohedron.

The n-diagram of W is the decomposition of the unit sphere into vertices, tie lines, and tie regions induced by the generalized Gauss map on W. For polyhedral W as we have here, the vertices of the n-diagram are the normals of faces of W, the

tie lines are the generalized Gauss map of edges of W and are the closed shorter great circle arcs connecting the two vertices which correspond to the faces of W meeting along that edge, and the tie regions are the generalized Gauss maps of the corners of W and are the closed regions of area less than 2π enclosed by the tie lines corresponding to the edges of W meeting at that corner. If more than three faces meet at some corner of W, then the corresponding tie region is not a tie triangle; the great circle segments which are not tie lines but which connect vertices of a tie region and lie within tie regions are called *extra lines* of the n-diagram. See [T2] or [TC] for more information, and see Fig. 1 for an example of an n-diagram for a generalized zonohedron and a Wulff shape with that n-diagram. W being a generalized zonohedron is equivalent to the property that the union of all tie lines of the n-diagram consists of a collection of complete great circles; these great circles triangulate the sphere when three faces meet at each corner of W.

We define a **subregion** of the n-diagram of W to be any spherical region which lies in a single tie region of the n-diagram and which is bounded by complete (noncrossing) tie lines or extra lines; there are subregions that are not tie regions when more than three faces meet at some vertex of W. Let A be the area of the largest tie region and a the area of the smallest tie region or subregion.

3. Local Structure

All embedded Φ-minimizing cones with boundary on the unit sphere and center at the origin and consisting of a finite number of plane segments, the normal of each of which is a vertex of the n-diagram corresponding to Φ, were catalogued in [T2] and [TC]. By hypothesis H1, any S considered in this paper can have only these as its possible local interior structures. For the convenience of the reader, we review here that catalog and the two properties implied by Φ-minimization used to derive it. We also prove a lemma which shows that we need to consider only some types of type-12 modification under the hypotheses of this paper.

The cones all consist of a finite number of plane segments, which here are called wedges. The **wedge** of an edge E of S is the wedge following (in the natural orientation of the cone) the corresponding edge in the tangent cone to S at V.

A cone of type 1 is a single plane segment, whose oriented unit normal is a vertex of the n-diagram. The standard cone of type 2 consists of two half-disks, being a tangent cone at an edge of either W or the central inversion of W (oriented so that the normals point inward). In the former case the two plane segments are said to meet along a **regular** edge, and in the latter they are said to meet along an **inverse** edge. In case W has more than three faces meeting at a vertex, there are extra type-2 cones, consisting of a pair of half-disks whose directions are vertices of a single tie region of the n-diagram but are not the endpoints of a tie line; as in the standard case, those that are *regular* meet in such a fashion that when the cone is translated to the corresponding corner of W, W lies entirely behind that translated cone, and those that are *inverse* have the central inversion of W lying entirely in front the appropriate translation of the cone. However, extra *inverse* type-2 cones are excluded from S by hypothesis H2. (They are minimizing but not volume maximizing among minimizing surfaces.)

The remaining cones of the catalog are composed of wedges whose oriented unit normals are vertices of the n-diagram and which meet pairwise in type-2 cones, in either a *regular* or an *inverse* fashion. Since each edge thus maps to a tie line or extra line of the n-diagram, these cones can be described by means of their corresponding oriented cycles in the n-diagram labeled by edge types. For example, the fragment of a cycle consisting of $n_1 \xrightarrow{r} n_2 \xrightarrow{i} n_3$ describes a wedge of orientation n_2, intersecting a wedge of orientation n_1 along the ray with orientation $-n_1 \times n_2$ (negative since the "r" denotes a *regular* edge) and a wedge of orientation n_3 along the ray $n_2 \times n_3$ (positive since the "i" denotes an *inverse* edge). A crucial fact is that these cycles turn out to bound currents on the sphere which are one or more complete subregions of the n-diagram, negatively oriented, except in the cases where the corresponding cone is a type-12 modification or a type-11 modification involving extra edges. When only three faces meet at each vertex of W, then there are no extra edges and no type-12 cones, when additionally W is a generalized zonohedron, only cones of the types 3, 4, 6, 8, 9, and 11 can occur as corners; typical examples of these types of cones are shown in Fig. 4 for the W of Fig. 1, along with their corresponding cycles on the n-diagram.

The only convex corners in the catalog are type-3 corners. If W has only three faces meeting at each vertex, then every such convex corner is a (translation of a) tangent cone to W. If W has more than three faces meeting at a vertex, then additional completely convex type-3 cones are possible: the directions of the wedges must be entirely from one tie region of the n-diagram and the wedges must occur in the same order as the corresponding vertices do around that tie region. (All other type-3 corners are forbidden in S by hypothesis H2.)

Type-4 and -5 cones consist of three wedges; two of the edges are *regular* and the other *inverse*, or vice versa, and the plane segment having two edges of the same

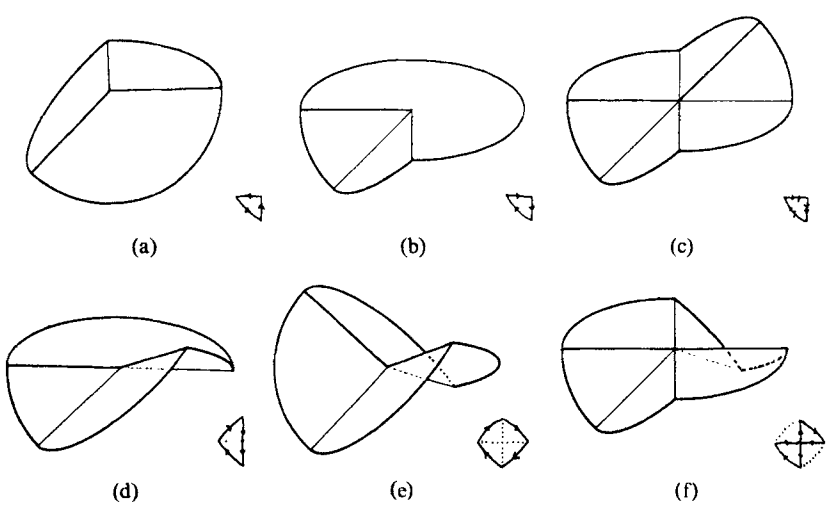

Fig. 4. Examples of possible interior corners and their corresponding Gauss maps for surfaces satisfying H1: (a) type 3, (b) type 4, (c) type 6, (d) type 8, (e) type 9, (f) type 11.

type is nonconvex. Type-6 and -7 cones consist of six wedges, with edge types alternating; their cycles consist of overlapping triangles in the n-diagram and all the wedges are convex. Type-8 and -9 cones consist of four wedges, with edge types alternating. Type-10 cones have five wedges, one of which is a half-disk with both edges being of the same type and the other plane segment being convex with different edge types; the corresponding cycle goes around a triangle on the n-diagram and then into the interior of the triangle and back out. Type-11 cones are modifications of previously defined cones and result from replacing an edge in the cycle by two edges, with the same type as the replaced edge, in such a way that parts of the two wedges in the cone corresponding to the vertices of the original edge are cut off and replaced by a convex wedge corresponding to the newly inserted vertex. All three directions must be in one tie region (by minimality); it is only when the replacing edges are extra lines (and thus, under the hypotheses of this paper, labeled *regular*) and they cross another edge of the cycle that the cycle does not bound a current consisting of complete subregions, all negatively oriented.

Type-12 cones also result from modifying previously defined cones. In this case one edge is replaced by three, with the outer two of those edges having their images in the n-diagram being extra edges which cross each other. Further requirements are that the outer two edges lie "inside" the two edges originally adjacent to the replaced edge (that is, that the angle α defined in the next section be smaller than that prior to modification at each end of the replaced edge), and that the number of nonconvex wedges in the cycle not be increased; also, if either vertex at an end of the original edge was convex even, then its nonreplaced edge must be part of the same tie region which contains the three new edges.

Lemma 1. *Any type-*12 *modification satisfying hypothesis* H2 *can be obtained by replacing a* regular *edge by three edges, the outer two being* regular *and the inner one* inverse. *Furthermore, a convex even wedge is never converted to a nonconvex even wedge by such a modification.*

Proof. The proof is left to the reader. We remark, however, that although we can construct type-12 modifications which involve replacing an edge labeled *inverse*, the condition that the number of nonconvex wedges not be increased implies that the same cone can arise by starting with a different cone, where the corresponding edge is *regular*, and replacing that edge. In particular, type-12 modifications of all-inverse type-3 corners are not allowed, by the property that the number of nonconvex wedges is not to be increased plus the property that any edge corresponding to an extra line in the n-diagram must be labeled *regular*. □

The catalog was derived using the two major consequences of the assumption of Φ-minimality, called Property 1 and Property 2 in Section 4 of [T2]. The first is that the normals of any two adjacent oriented wedges (i.e., wedges with a common line segment) must be vertices from a single tie region of the n-diagram (and thus correspond to a tie line or extra line), and the second is that convex wedges with both edges being *regular* or both being *inverse* must have the normal of that wedge and its two adjacent wedges be vertices of a single tie region (see p. 393 of [T2]).

These two properties are also assumed in H1 and are used in the very partial classification of possible corners at the boundary B of S which must be proved in Proposition 2(d) under hypothesis HZ.

4. Notation

For examples of the definitions in this section, see the examples and associated figures (particularly Fig. 7) in Section 6.

4.1. Parts of S

The boundary of a plane segment P can be decomposed into one or more connected cycles, but not uniquely when these cycles are not disjoint simple closed curves. To obtain uniqueness and the properties we will need, we require the decomposition into cycles to have the property that for each pair of successive edges in a cycle, there is a single wedge of P partially bounded by those two edges. Let $1 + g(P)$ be the number of cycles in the boundary of P, assuming that the decomposition has this property.

The set of all plane segments of S is denoted by $\mathscr{P}$; S is the union of its plane segments.

Let $\mathscr{C}(I)$ denote the set of interior corners of S. We use the word "corner" rather than vertex to emphasize that more than two plane segments meet at a corner. Let $\mathscr{V}_3$ denote the set of type-3 corners in S or type-12 modifications of them, and let $\mathscr{V}_{12}$ denote the set of type-12 corners in S (see Section 3).

Let $\mathscr{C}_3$ denote the set of points of S which are in the interior of a line segment of B and contained in more than one (and thus three or more) plane segments of S.

The union of the interior corners, the corners of B and the corners in $\mathscr{C}_3$ are the points geometrically required to be corners of S. For purposes of the proofs of this paper, it is convenient to require S to have one and only one more type of corner. The images of the line segments of B are partitioned into intervals by the images of the elements in the union of the corners of B and the points in $\mathscr{C}_3$; we let the inverse images of the midpoints of these intervals in the corresponding parts of the boundary of S be denoted corners as well and let the union of these "midpoint corners" be denoted $\mathscr{C}_0$. We include these midpoint corners because the rules given below for labeling edges on the boundary of S are naturally determined to each side of the corners in $\mathscr{C}_3$ and the corners of B which are contained in more than one plane segment, and these rules can be different for the different ends of a single interval in B.

It is also convenient to divide the corners of B into two classes and to isolate a particular subclass of one of these classes. We thus let $\mathscr{C}_1$ be the set of corners of B which are contained in only one plane segment and let $\mathscr{C}_2$ be the remaining corners of B. We let $\mathscr{C}_{1'}$ be the set of "last" corners in $\mathscr{C}_1$ — that is, those corners in $\mathscr{C}_1$ which are not immediately followed (after the appropriate midpoint corner) by another corner in $\mathscr{C}_1$.

The **corners of** S are thus the union of the elements of $\mathscr{C}(I)$, $\mathscr{C}_0$, $\mathscr{C}_1$, $\mathscr{C}_2$, and $\mathscr{C}_3$; the set of all corners is denoted $\mathscr{C}$, and the set of corners not in $\mathscr{C}(I)$ is denoted $\mathscr{C}(B)$.

The edges of S are now naturally defined, given the requirements on the plane segments and corners of S, except that we will find it convenient to deal exclusively with oriented edges. Thus E is an **edge of** S if and only if E is part of the oriented boundary of some plane segment of S, the boundary of E consists of two corners of S, and E contains no other corners of S. The final corner of E is denoted as $V(E)$ and the initial one as $V_i(E)$. Note that not only does E determine a unique such final and initial corner, but that it also determines a unique plane segment $P(E)$ for which it is part of an oriented boundary and, unless E is part of the boundary of S, another unique plane segment $P_i(E)$ for which it is part of the boundary with reversed orientation. To each edge E we can associate a unit vector $v(E)$, the vector directing (the image of) E. (In Tables 2 and 3, we use the notation $v(V)$ for $v(E)$ when $V = V(E)$ is in $\mathscr{C}_2 \cup \mathscr{C}_3$.) It is also convenient, in this section and in Proposition 5, to associate to each E the edge $E_+(E)$, defined to be the edge immediately following E in the appropriate cycle of the boundary of $P(E)$.

Let $\mathscr{E}$ denote the set of all oriented edges of S, let $\mathscr{E}(B)$ denote the set of edges of S contained in the boundary of S, and let $\mathscr{E}(I) = \mathscr{E} \sim \mathscr{E}(B)$. It is convenient to have a notation for the set of edges E such that $V(E) = V$ for a given $V \in \mathscr{C}$; let $\Gamma(V)$ be that set. Let $\mathscr{E}_3$ be the set of edges such that $V(E) \in \mathscr{V}_3$ and E and $E_+(E)$ are both labeled *regular*.

For Proposition 5 and following, the following notation will be useful: for $V \in \mathscr{C}_2 \cup \mathscr{C}_3$, $E'(V)$ is the edge in $\mathscr{E}(B)$ preceding the edge $E \in \mathscr{E}(B)$ for which $V = V(E)$, so that $V(E_+(E'(V))) = V$; for $V \in \mathscr{C}_1$, $E'(V) \in \mathscr{E}(B)$ is the edge such that $V = V_i(E'(V))$.

Note that in our notation the Euler characteristic $\chi(S)$ is given by

$$\chi(S) = card(\mathscr{P}) - \sum_{P \in \mathscr{P}} g(P) + card(\mathscr{C}) - (card(\mathscr{E}) - card(\mathscr{E}(B)))/2 - card(\mathscr{E}(B))$$

since the decomposition of S into plane segments, unoriented edges, and corners gives a polyhedral cell decomposition of S.

Throughout the rest of this paper (and in particular for the definitions that follow) we require that S satisfy conditions S1, H1, H2, and H3.

4.2. Gauss Maps

The Gauss maps, and thereby the Gauss curvatures, are relatively straightforward and standard to define on the interior of S (though this is not the case when S is not locally embedded!). However, things are not so obvious on the boundary. Furthermore, the fact that the Gauss maps come in predefined "quanta" or chunks of the sphere is crucial to the results of this paper and it is only seen by examining the Gauss map in some detail. Finally, the definitions of the angles α, central to Proposition 5, will depend on the Gauss maps of the edges (in the boundary of S as well as in the interior). Therefore we will specify these Gauss maps fairly carefully.

We use the notation ν throughout for the Gauss map; we subscript it in its

various guises to emphasize the fact that it is a zero-, one- or two-dimensional current (subset of the sphere with orientation and multiplicity).

For each $P \in \mathscr{P}$, define $v_0(P)$ to be the oriented unit normal of the plane corresponding to P. By hypothesis H1, this unit normal is a vertex of the n-diagram of W.

For each $E \in \mathscr{E}(I)$, define $v_1(E)$ to be the oriented shorter great circle segment from $P(E)$ to $P_i(E)$. By hypothesis H1, $v_1(E)$ is an oriented tie line or extra line of the n-diagram of W.

For each interior corner V, $\Sigma_{E \in \Gamma(V)} v_1(E)$ is a cycle on the n-diagram. If V is type 3 (a convex corner), then this cycle bounds a tie region or part of a tie region of positive orientation; let $v_2(V)$ be this region and let $K(V)$ be the area of the region. Note that $K(V) \leq A$. If V is type 4, 5, 8, 9, or 10, then the cycle bounds a region of negative orientation (triangular, in the first two cases) composed of tie regions; define $v_2(V)$ to be this region and define $K(V)$ to be the negative of its area. If V is type 6 or 7, then the cycle bounds two overlapping triangles of negative orientation; let $v_2(V)$ be the sum of these two negatively oriented regions and let $K(V)$ be the negative of the sum of their areas. Note that for types 4–10, v_2 is composed of one or more subregions of the n-diagram and thus $K(V) \leq -a$.

If V is a type-11 modification of one of these types, then normally the effect for each such modification is to remove a tie triangle or subregion from the Gauss map of V, and thus to subtract the negative of the area of that triangle from $K(V)$. However, if some tie region of the n-diagram contains five or more vertices, it is possible for the modification to consist, when described in terms of its effect on the cycle in this n-diagram, of replacing a single *regular* edge (extra or not) by a pair of extra *regular* edges, and these edges may cross some other extra *regular* edge of the cycle. In this case, $v_2(V)$ may have a region of positive orientation, and we only know that $K(V)$ is less than A times the number of these awkward type-11 modifications. We thus let $\mathscr{E}_{a11}$ be the set of oriented edges such that the wedge of $P(E)$ at $V(E)$ comes from one of these awkward type-11 modifications, and know that we will have to make a special effort to count these edges. We also let $\mathscr{V}_{a11}$ be the set of corners V such that $V = V(E)$ for some $E \in \mathscr{E}_{a11}$.

If V is a type-12 corner, then for each type-12 modification a triangle of positive orientation and one of negative orientation must be added to make the corresponding modification to v_2. The areas of these regions must be respectively added to and subtracted from the $K(V)$'s. This may result in some regions of the sphere having positive orientation. Note, however, that for any such modification, the triangle of positive orientation is contained inside a single tie region.

We complete the definition of interior quantities by defining $m(V)$ to be 1 if V is a type-6 or -7 corner or a type-11 modification of such a corner, $m(V) = 0$ if V is any other interior corner not in $\mathscr{V}_{12}$, and we define $m(V)$ for type-12 corners by starting with a value of $m(V)$ appropriate to the basic corner type and adding 1 for each type-12 modification of it. Thus $m(V) > 0$ if and only if the Gauss map of V has a branch point for corners of type 4–11, and $m(V) > 0$ for each type-12 corner.

We now turn to the boundary.

By definition, each V in $\mathscr{C}_2$ is in two edges in $\mathscr{E}(B)$; let E be the first (so $V = V(E)$) and F the next. Define $v_0(V)$ to be the unit vector in the direction of $v(E) \times v(F)$. Thus if there were a convex piece of a plane having these two line

segments of B as part of its boundary, it would have normal $v_0(V)$. (It is possible to define phantom plane segments in the corners, but this device of assigning a direction to a corner vertex works more easily.)

For each V in $\mathscr{C}_1 \cup \mathscr{C}_0$, define $v_0(V)$ to be $v_0(P)$ for the unique plane segment P of S containing V.

We define $v_1(E)$ only for some edges in $\mathscr{E}(B)$; on these noninterior edges v_1 need not be a tie line but it is always a great circle segment in the plane perpendicular to $v(E)$, the vector orienting the edge. (It is not absolutely necessary to define v_1 on edges in $\mathscr{E}(B)$, but it is useful in that it gives a geometric meaning to the angles α defined below.) For $E \in \mathscr{E}(B)$ with $V(E)$ (resp. $V_i(E)$) in $\mathscr{C}_2$, define $v_1(E)$ to be the shorter great circle segment (if it is uniquely defined) from $v_0(P(E))$ to $v_0(V(E))$ (resp. from $v_0(V(E))$ to $v_0(P(E)$. If v_1 remains undefined on both of the boundary edges containing a V in $\mathscr{C}_2$, then their adjacent planes have the same value of v_0, and v_1 need not be defined on those edges. Otherwise, for only one E in $\mathscr{E}(B)$ containing V is $v_0(P(E))$ antipodal to $v_0(V)$. If V is $V(E)$, let $v_1(E)$ be the half-circle so that the angle at $v_0(V)$ from that half-circle to v_1 of the other edge is less than π, and orient it so that $v_0(V)$ is its final corner. If V is $V_i(E)$, then let $v_1(E)$ be the half-circle so that the angle from v_1 of the other edge to it is less than π and orient it so that $v_0(V)$ is its initial corner.

For V in $\mathscr{C}_0$ or $\mathscr{C}_1$, define $K(V)$ to be zero (and, for consistency, define $v_2(V)$ to be the zero two-dimensional integral current). For V in $\mathscr{C}_2$ such that there are only two plane segments of S containing V, there is a unique interior edge E with $V = V(E)$, as well as two boundary edges E' and E'' containing V, and $v_1(E) + v_1(E') + v_1(E'')$ is a cycle on the sphere. Let $v_2(V)$ be the negatively oriented spherical triangle bounded by this cycle, and let $K(V)$ be the negative of its area. For all remaining V in $\mathscr{C}(B)$, just define

$$K(V) = -\kappa(V) - \sum_{E \in \Gamma(V)} \gamma(E) + \pi,$$

where κ and γ are defined below; leave $v_2(V)$ undefined. (There are geometric ways of defining the Gauss curvature at these more complicated corners, but they can get pretty involved, and this is the formula that we need to have hold eventually anyway.)

Define $m(V) = 0$ for each V in $\mathscr{C}(B)$.

4.3. *Angles and Edge Labels (κ, n, α, and γ)*

We define the exterior angles of the boundary B in the natural way: For V in $\mathscr{C}_0$ or $\mathscr{C}_3$, define $\kappa(V) = 0$. For each V in $\mathscr{C}_2$, define $\kappa(V)$ to be the angle between $v(E)$ and $v(F)$, where E, F are the edges in $\mathscr{E}(B)$ containing V (so that $0 < \kappa(V) < \pi$). For V in $\mathscr{C}_1$, define $\kappa(V)$ to be the exterior angle of the boundary B at V in the oriented plane segment containing V. Note that $\kappa(V) + K(V)$ is the true geodesic curvature of B in S at V.

For each E in $\mathscr{E}(I)$, define *Label*(E) to be *regular* or *inverse* according to whether the plane segments $P(E)$ and $P_i(E)$ make a *regular* or *inverse* union along E (that is,

according to whether that union is like that of a tangent cone to W or to its central inversion; see Section 3). Once again, we have to be careful at the boundary: for E in $\mathscr{E}(B)$ with $V(E)$ (resp. $V_i(E)$) in $\mathscr{C}_2$ or $\mathscr{C}_3$, define *Label*(E) to be the opposite of *Label*$(E_+(E))$ (resp. the opposite of the label of the edge immediately preceding E in a cycle of the boundary of $P(E)$). For all remaining edges in $\mathscr{E}(B)$, define *Label*(E) to be the same as the label of the last edge in $\mathscr{E}(B)$ preceding E for which *Label* is defined. Note that both edges to any corner in C_1 have the same label, and that the label can change at a corner in C_0 only if that corner immediately precedes a corner in $\mathscr{C}_2$ or $\mathscr{C}_3$.

For each E in $\mathscr{E}$, define $\gamma(E)$ to be the angle of the wedge of $P(E)$ containing E at $V(E)$, so that $\pi - \gamma(E)$ is the exterior angle of that wedge at $V(E)$.

If neither E nor $E_+(E)$ is in $\mathscr{E}(B)$, define $\alpha(E)$ to be the angle, between 0 and 2π, at $v_0(P(E))$ from $v_1(E_+(E))$ to $v_1(E)$, unless those geodesics coincide along at least part of their lengths; in that case define $\alpha(E)$ to be 2π if $v_2(V(E))$ is defined and covers a neighborhood of $v_0(P(E))$ and 0 otherwise. If $V(E) \in \mathscr{C}_1$, define $\alpha(E) = \gamma(E) - \pi$. If $V(E) \in \mathscr{C}_0$, define $\alpha(E)$ to be 0 if *Label*$(E) =$ *Label*$(E_+(E))$ and π otherwise. If $V(E) \in \mathscr{C}_2 \cup \mathscr{C}_3$ and E or $E_+(E)$ is in $\mathscr{E}(B)$, then define $\alpha(E) = \gamma(E)$. The object is to ensure that α is the angle of the Gauss map of $P(E)$ at $V(E)$, if that Gauss map is defined.

Finally, we want to define a number which indicates whether *Label* changes (or "ought" to change) in going from E to $E_+(E)$ or not. For each E in $\mathscr{E}$, we thus define $n(E)$ to be 1 if *Label* does so change. However, we define $n(E) = 2$, rather than 0, when *Label* does not change provided $\alpha(E) \geq \pi$ and $V \notin \mathscr{V}_3$ and $V(E)$ is not in $\mathscr{C}_0$ (and define $n(E) = 0$ otherwise). If $n = 2$, then a small change in the position of the plane segments at $V(E)$ can introduce new edges with the opposite edge type, so n is the number of times the edge label "should" change in going from E to $E_+(E)$. Note that $\alpha(E) = \gamma(E)$ whenever $n(E) = 1$, that $\alpha(E) = \gamma(E) - \pi$ if $n(E) = 0$ and $V \notin \mathscr{V}_3$, and that $\alpha(E) = \gamma(E) + \pi$ if $n(E) = 0$ and $V \in \mathscr{V}_3$ or if $n(E) = 2$.

5. Results

Proposition 2.

(a) *For each* $P \in \mathscr{P}$,

$$\sum_{E \in p_0(P)} (\pi - \gamma(E)) - 2\pi(1 - g(P)) = 0.$$

(b) *For each* $V \in \mathscr{C}(I)$,

$$K(V) - 2\pi + \sum_{E \in \Gamma(V)} \gamma(E) = 0$$

and, for each $V \in \mathscr{C}(B)$,

$$K(V) - 2\pi + \sum_{E \in \Gamma(V)} \gamma(E) + \pi + \kappa(V) = 0.$$

(c)

$$\sum_{E\in\Gamma(V)}(1-n(E)/2)-2\begin{cases}\geq 1+m(V) & \text{if } V\in\mathscr{V}_3,\\ =m(V) & \text{if } V\in\mathscr{C}(I)\sim\mathscr{V}_3,\\ =-1 & \text{if } V\in\mathscr{C}_1,\\ \geq -1 & \text{if } V\in\mathscr{C}_2,\\ \geq -\frac{1}{2} & \text{if } V\in\mathscr{C}_3,\\ =-1 & \text{if } V\in\mathscr{C}_0 \text{ and } n(E)=0 \text{ for the } E\in\Gamma(V),\\ =-\frac{3}{2} & \text{if } V\in\mathscr{C}_0 \text{ and } n(E)=1 \text{ for the } E\in\Gamma(V),\end{cases}$$

and, when $V\in\mathscr{C}_2$, *equality holds if there are exactly two elements in* $\Gamma(V)$.

(d) If $V\in\mathscr{V}_3\sim\mathscr{V}_{12}$, *then* $K(V)\leq A$ *and* $v_2(V)$ *is a union of subregions from a single tie region of the n-diagram. If* $V\in\mathscr{V}_{12}$, *then* $K(V)<Am(V)$ *and* $m(V)\geq 1$. *If* $V\in\mathscr{V}_{a11}$, *then* $K(V)<A\ \mathrm{card}\{E\in\mathscr{E}_{a11}: V(E)=V\}$.

If $V\in\mathscr{C}(I)\sim(\mathscr{V}_3\cup\mathscr{V}_{12}\cup\mathscr{V}_{a11})$, *then* $K(V)\leq -a$ *and* $v_2(V)$ *is composed of one or more subregions of the n-diagram.*

If $V\in\mathscr{C}_2\cup\mathscr{C}_3$, *then* $K(V)<0$, *and whenever equality holds in* (c) *above and* HZ *holds and* $V\in\mathscr{C}_3$, $K(V)\leq -a$.

If $V\in\mathscr{C}_0\cup\mathscr{C}_1$, *then* $K(V)=0$.

Proof. (a) This is the classical Gauss-Bonnet theorem for P, since the immersion of P has no branch points and no interior curvature.

(b) For $V\in\mathscr{C}(I)$, the statement in (b) is a result of the Gauss-Bonnet theorem, since S is locally embedded and for small enough $\delta>0$ the exterior angle of the boundary of $S\cap\{x: |x-V|\leq\delta\}$ is $\gamma(E)$ within each $P(E)$ for which $E\in\Gamma(V)$ and 0 at each intersection between wedges. (Alternatively, we could apply the Gauss-Bonnet theorem to the mapping $v_2(V)$.)

If $V\in\mathscr{C}_2$ and $\Gamma(V)$ has only two edges, then $v_2(V)$ is defined and is a spherical triangle with negative orientation. The assertion of part (b) follows from applying the Gauss-Bonnet theorem to $v_2(V)$ with positive orientation on the sphere (so that its curvature is $|K(V)|=-K(\mathrm{V})$), since then the geodesic curvature of $\partial v_2(V)$ at $v_0(V)$ is $\pi-\kappa(V)$ and at $v_0(P(E))$ is $\pi-\alpha(E)$ for each E in $\Gamma(V)$, and $\alpha(E)=\gamma(E)$ when $n(E)=1$.

For all remaining corners in $\mathscr{C}(B)$, the statement in (b) follows immediately from the definition of $K(V)$ and $\kappa(V)$.

(c) From the catalog of corners and hypothesis H2, we know that, for $V\in\mathscr{V}_3\sim\mathscr{V}_{12}$, all edges in $\Gamma(V)$ are labeled *regular* and there are at least three plane segment wedges at V (exactly three if the tie lines in the n-diagram triangulate the sphere) and each is convex; thus $n(E)=0$ for each such E. Each type-12 modification adds two edges with $n(E)=1$ and thus 1 to the sum; the first bound follows. For $V\in\mathscr{C}(I)\sim\mathscr{V}_3$, the equality likewise follows from the description of the corners in the catalog and the definition of n and m. For $V\in\mathscr{C}_1\cup\mathscr{C}_0$,

there is only one edge in $\Gamma(V)$, and the equalities are immediate from the definition of n and the labels on edges in $\mathscr{E}(B)$.

For V in $\mathscr{C}_2$ or $\mathscr{C}_3$, *Label* was defined on edges in $\mathscr{E}(B)$ so that $n(E_i) = 1$ for the edge E_1 in $\mathscr{E}(B)$ for which $V(E_1) = V$ and for the edge E_2 in $\mathscr{E}(I)$ for which $V(E_2) = V$, so the left-hand side is automatically at least -1 and equals -1 in case there are only those two edges in $\Gamma(V)$.

We claim that for $V \in \mathscr{C}_3$, local embeddedness implies that there is at least one additional edge E in $\Gamma(V)$ with $n(E) > 0$, and thus that the left-hand side is at least $-\frac{1}{2}$. By hypothesis H1, if $n(E) = 2$ for some E in $\Gamma(V)$, then $P(E)$ and the two plane segments adjacent to it have as their normals the vertices of a single tie region; thus all directions of plane segments at such a corner would have to lie in the same tie region of the n-diagram. We can now construct such cones where there are only $n(E) = 2$ wedges between $P(E_1)$ and $P(E_2)$, and see that in these cones two wedges must intersect, contradicting local embeddedness. In particular, assume without loss of generality that all interior edges at V are labeled *regular*, and let $n_1 = v_0(P_1)$. Let n_0 denote a unit vector such that $v(E_1) = c(n_1 \times n_0)$ for some $c > 0$. Note that this implies that n_0 is on the great circle corresponding to the boundary line segment containing V, and that the image of E_1 is that of the labeled cycle fragment $n_1 \overset{r}{\to} n_0$, as defined in Section 3. By embeddedness, the image of P_1 cannot contain any of the image of the boundary line segment on the other side of V. Thus $\gamma(E_1)$ must be less than π, and thus n_0 lies on a specific side of the great circle containing the tie line or extra line corresponding to the edge in $P(E_1)$ following E_1. The same considerations apply to $P(E_2)$ and a direction n_0', leading to the conclusion that either the shorter great circle segment from n_1 to n_0 intersects the interior of the tie region, or the shorter great circle arc from n_0' to $v_0(P(E_2))$ does. If $n_1 = v_0(P(E_2))$, then $n_0 = n_0'$ and this position of n_0 implies that both wedges must contain at least the wedge corresponding to $s \overset{r}{\to} n_1 \overset{r}{\to} t$, where in the tie region, positively oriented, is the vertex immediately preceding n_1 and t is the vertex immediately following it. This means that they overlap, a contradiction of embeddedness. If $n_1 \neq v_0(P(E_2))$, we treat the case that the arc from n_1 to n_0 is inside; the other case is similar. Thus $P(E_1)$ is a relatively fat wedge; it contains the rays corresponding to $n_1 \overset{r}{\to} x$ for each vertex x in the tie region which is on the other side of the boundary-line great circle from the direction w of its adjacent wedge at V. The wedge Y next to $P(E_2)$ is similarly fairly large, as it contains the rays corresponding to $z \overset{r}{\to} y$, for y the direction of Y and z any vertex on the same side as n_1 of the great circle through y and $v_0(P(E_2))$. (The fact that $\gamma(E_2) < \pi$ implies that y and w are on opposite sides of the great circle corresponding to the boundary line segment.) In particular, both wedges Y and $P(E_1)$ contain the ray $n_1 \overset{r}{\to} y$, and thus $P(E_1)$ and the wedge adjacent to $P(E_2)$ intersect. Since these two wedges are not themselves adjacent, this contradicts embeddedness. (See the Comment below for further discussion of this case; the construction of cones corresponding to labeled cycles is given in detail in [T2].)

(d) The assertions for $V \in \mathscr{C}(I)$ follow directly from the catalog and the resulting natural definition of K, as described in Section 4. On the other hand, this is the key property that makes the *a priori* bound of this paper work.

$K(V) = 0$ for $V \in \mathscr{C}_0 \cup \mathscr{C}_1$ by definition.

Suppose that $V \in \mathscr{C}_2$ and that $\Gamma(V)$ has only two members, E_1 and E_2 with $E_1 \in \mathscr{E}(B)$. (Note that the edge $F \in \mathscr{E}(B)$ such that $V_i(F) = V$ is not in $\Gamma(V)$.) Then $v_2(V)$ is a spherical triangle with negative orientation, and so automatically $K(V) < 0$. If $v_1(E_1)$ and $v_1(F)$ are each composed of one or more tie lines of the n-diagram (as is the case under assumption HZ), then $v_2(V)$ is composed of one or more tie regions and so $K(V) \leq -a$

If $V \in \mathscr{C}_2$ and $\Gamma(V)$ has more than two members, then the statement $K(V) < 0$ is equivalent to $\sum_{E \in \Gamma(V)} \gamma(E) > \pi - \kappa(V)$, which holds because the right-hand side is the angle of a convex plane segment in that corner of B whereas the left-hand side is the sum of the angles of wedges spanning the same corner.

Finally we examine the case $V \in \mathscr{C}_3$. Here, $K(V) < 0$ if and only if $\sum_{E \in \Gamma(V)} \gamma(E) > \pi$. But this must always be true, since the union of the wedges of the plane segments at V must span the straight line segment made by the two edges E_1 and F in $\mathscr{C}(B)$ containing V.

In order for equality to hold in (c), there must be one additional edge E_3 with $n(E_3) = 1$ and n must be 2 on all other edges. We will show that this would imply that $K(V)$ is the negative of the area of a region of the sphere which is bounded by tie lines ($\sum v_1(E)$, where the sum is over all E in $\Gamma(V)$ except E_1) and one of the two portions bounded by $v_0(P(E_1))$ and $v_0(P(E_2))$ of the great circle C perpendicular to $v(E_1)$.

As in the proofs above, $n(E) = 2$ implies that $P(E)$ and the two plane segments adjacent to it have as their normals the vertices of a single tie region. By local embeddedness, the directions of a sequence of plane wedges at V meeting along $n = 2$ edges travel around the vertices of the tie region at most once. (As above, we can show that a repeated direction leads to an overlap of those plane segments, since they must each contain a minimum-size wedge; if extra edges of the cycle cross in the n-diagram, then we show that a specified ray is contained in each of two wedges, proving self-intersection.)

Suppose first that $v_0(P(E_1)) \neq v_0(P(E_3)) \neq v_0(P(E_2))$. Whether there are wedges on each side or not, hypothesis H1 implies that there must be a tie line in the n-diagram between $v_0(P(E_3))$ and $v_0(P(E_1))$ and between $v_0(P(E_3))$ and $v_0(P(E_2))$. By local embeddedness again, $v_0(P(E_1)) \neq v_0(P(E_2))$. One of the two portions of C with these two endpoints makes angle $\alpha(E_1)$ with $v_1(E_1)$: we check that it also makes angle $\alpha(E_2)$ with $v_1(E_2)$. (Note that this might be the longer portion of C). This portion of C, appropriately oriented, together with $v_1(E_1)$ and $v_1(E_2)$, bounds a spherical triangle with negative orientation. If there were no edges in $\Gamma(V)$ with $n = 2$, then we see that the Gauss–Bonnet theorem requires that $|K(V)|$ be the area of this spherical triangle. If $n = 2$ wedges are also present on one or both sides, the area(s) of the appropriate union of subregions of the tie region(s) must be subtracted from the area of the spherical triangle with vertices $\{v_0(P(E_3)), v_0(P(E_2)), v_0(P(E_1))\}$ to give $|K(V)|$.

We are left with the case that $v_0(P(E_3)) = v_0(P(E_1))$ and/or $v_0(P(E_3)) = v_0(P(E_2))$; suppose without loss of generality that $v_0(P(E_3)) = v_0(P(E_1))$; by hypothesis H2, that direction together with the directions of the intervening wedges are vertices of a tie region of the n-diagram. Local embeddedness now implies that

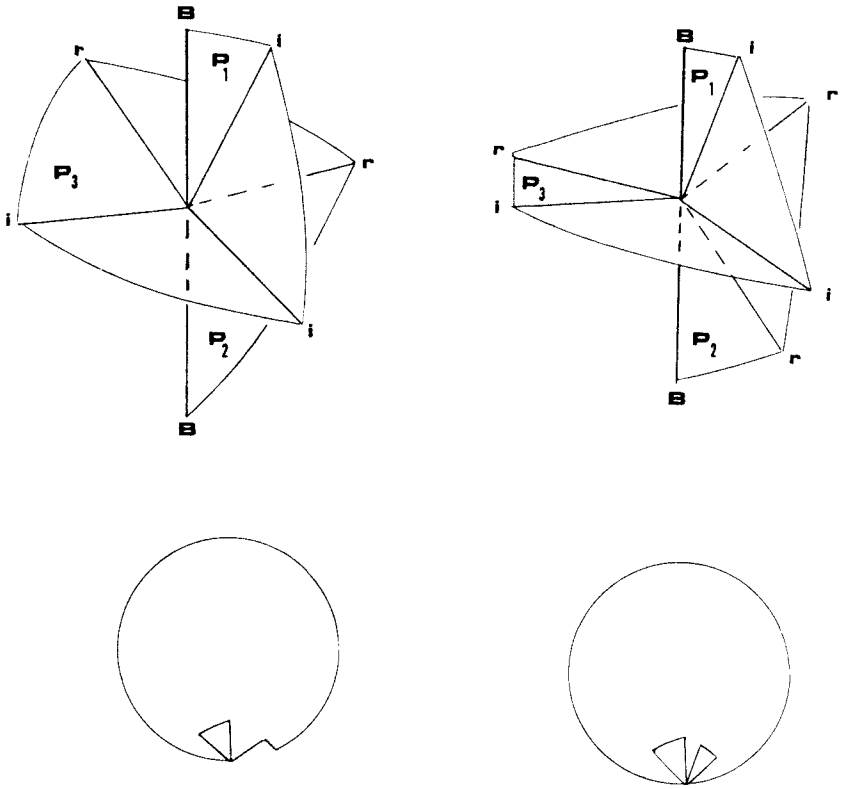

Fig. 5. Examples of two types of embedded corners which can occur along the boundary B in surfaces satisfying H1, together with their associated Gauss maps.

the situation must be one of the two sketched in Fig. 5. Thus there is a region of the sphere, negatively oriented, bounded by the longer portion of C (or all of C, in case also $v_0(P(E_3)) = v_0(P(E_2))$) plus the sum, over all edges E in $\Gamma(V)$ except E_1, of $v_1(E)$; this region is a hemisphere less two tie regions or portions thereof. Since the angles $\alpha(E)$, for all E in $\Gamma(V)$, are precisely the interior angles of this region, the Gauss–Bonnet theorem once again tells us that the area of this region is $|K(V)|$.

Under hypothesis HZ, all the curves bounding this region lie within union of all tie lines or extra lines of the n-diagram, and thus the region is composed of one or more complete subregions, and has area at least a. In general, its curves lie on the tie lines and extra tie lines plus the great circle C, and thus its area is bounded below by a'. □

Comment. The delicacy of some of the definitions and arguments is illustrated by considering one of the nonembedded cones which arose in the proof of part (c), one where there are exactly three edges in $\Gamma(V)$ and $n(E_3) = 2$. This situation is illustrated in Fig. 6. Although this cone is nonembedded, it "just misses" being embedded, in that $P(E_2)$ intersects $P(E_1)$ only along one of its edges, and that edge

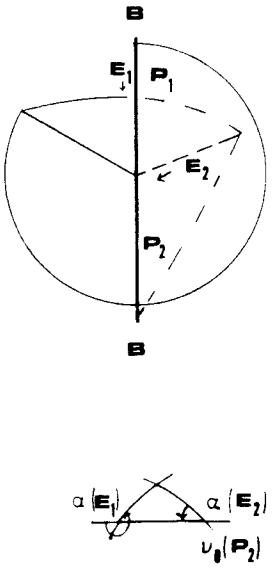

Fig. 6. An example of a (barely) nonembedded corner with a line segment of B as part of its boundary and with all edges having $n(E) = 0$ except for the two required by convention to have $n(E) = 1$; the relevant portion of the n-diagram is also indicated. See the Comment at the end of Proposition 2.

is in the boundary B; if that part of the boundary could be slightly moved, there would be no self-intersection (although then the corner would no longer be a candidate for a $\mathscr{C}_3$ corner). If we were to attempt to define a Gauss map for this corner, we would immediately run into difficulties, as neither portion of C would have both the correct angle $\alpha(E_1)$ at $\nu_0(P(E_1))$ and the correct angle $\alpha(E_2)$ at $\nu_0(P(E_2))$. Thus in order to handle the situation where S can have local self-intersections while preserving the useful notion of Gauss maps, we have to abandon the convenient labeling of edges in $\mathscr{E}(B)$ which ensures that $n(E_1) = 1 = n(E_2)$. But that is a problem for another paper.

Lemma 3. $\sum_{V \in \mathscr{C}} K(V) + \sum_{V \in \mathscr{C}(B)} \kappa(V) = 2\pi\chi(S)$.

Proof. This is essentially the Gauss–Bonnet theorem in this polyhedral context. We prove it here to show both that it applies to our types of polyhedral surfaces and that our definitions are consistent.

We sum the results of Proposition 2(a) and (b) over all P in $\mathscr{P}$ and all V in $\mathscr{C}$ and use the fact that $\sum_{P \in \mathscr{P}} \sum_{E \in \partial P} 1 = \sum_{V \in \mathscr{C}} \sum_{E \in \Gamma(V)} 1 = card(\mathscr{E})$ to obtain

$$\begin{aligned} 0 &= -2\pi\, card(\mathscr{P}) + 2\pi \sum_{\mathscr{P}} g(P) + \pi\, card(\mathscr{E}) \\ &\quad + \sum_{V \in \mathscr{C}} K(V) + \sum_{V \in \mathscr{C}(B)} \kappa(V) - 2\pi\, card(\mathscr{C}) + \pi\, card(\mathscr{E}(B)) \\ &= \sum_{V \in \mathscr{C}} K(V) + \sum_{V \in \mathscr{C}(B)} \kappa(V) - 2\pi\chi(S). \end{aligned}$$

□

Proposition 4.

$$\sum_{P\in\mathscr{P}}\left(2-\sum_{E\in\partial P} n(E)/2\right) \geq card(\mathscr{V}_3)+\sum_{V\in\mathscr{C}(I)} m(V)+2\chi(S)+2\sum_{\mathscr{P}} g(P)$$
$$-(\tfrac{1}{2})\,card\{V\in\mathscr{C}_0\colon n(E)=1\}+card(\mathscr{C}_3)$$
$$-(\tfrac{1}{2})\,card\{V\in\mathscr{C}_3\colon \textstyle\sum(1-n(E)/2)=\tfrac{3}{2}\}.$$

Proof. We look carefully at

$$\sum_{V\in\mathscr{C}}\left(\sum_{E\in\Gamma(V)}(1-n(E)/2)-2\right).$$

If we arrange it, it becomes

$$\sum_{P\in\mathscr{P}}\sum_{E\in\partial P} 1-\sum_{P\in\mathscr{P}}\sum_{E\in\partial P} n(E)/2-2\,card(\mathscr{C}),$$

which is in turn equal to

$$card(\mathscr{E})-2\,card(\mathscr{P})+\sum_{P\in\mathscr{P}}(2-\sum_{E\in\partial P} n(E)/2)-2\,card(\mathscr{C}).$$

Now we recognize most of $-2\chi(S)$; this expression is in fact equal to

$$-2\chi(S)-card(\mathscr{E}(B))-2\sum_{\mathscr{P}} g(P)+\sum_{P\in\mathscr{P}}(2-\sum_{E\in\partial P} n(E)/2).$$

But by part (c) of Proposition 2, the initial expression is at least as large as

$$card(\mathscr{V}_3)+\sum_{V\in\mathscr{C}(I)} m(V)-card(\mathscr{C}(B))+card(\mathscr{C}_3)$$
$$-(\tfrac{1}{2})\,card\{V\in\mathscr{C}_3\colon \textstyle\sum(1-n(E)/2)=\tfrac{3}{2}\}$$
$$-(\tfrac{1}{2})\,card\{V\in\mathscr{C}_0\colon n(E)=1\}.$$

Since $card(\mathscr{E}(B))=card(\mathscr{C}(B))$, we can rewrite this inequality as in the statement of the proposition. □

Proposition 5.

(a) *If* $g(P)\neq 0$, *then*

$$2-\sum_{E\in\partial P} n(E)/2\leq 2g(P).$$

(b) *If* $P \in \mathscr{P}$ *has* $g(P) = 0$, *and no edge in* ∂P *is in* $\mathscr{E}(B)$,

$$\begin{aligned} 1 - \sum_{E \in \partial P} n(E)/2 \\ &\leq card\{E \in \partial P: E \in \mathscr{E}_3\} - (1/2\pi) \sum_{E \in \partial P} \alpha(E) \\ &\leq -1 - card\{E \in \partial P: E \in \mathscr{E}_{a11}\}. \end{aligned}$$

(c) *For each* $P \in \mathscr{P}$ *with* $g(P) = 0$ *and with an edge in* $\partial P \cap \mathscr{E}(B)$, *let* $d = 0$ *if* $n(E) = 0$ *for all* E *such that* $V(E) \in \mathscr{C}_0 \cap \partial P$ *and* $d = 1$ *otherwise. Then*

$$\begin{aligned} 2(1 - g(P)) - \sum_{E \in \partial P} n(E)/2 \\ \leq \begin{cases} card\{V \in \mathscr{C}_{1l} \cap \partial P: n(E'(V)) = 0\} & \text{if HZ holds,} \\ 1 - d & \text{in general.} \end{cases} \end{aligned}$$

(*Recall that for* $V \in \mathscr{C}_1$, $E'(V) \in \mathscr{E}(B)$ *is the edge such that* $V = V_i(E'(V))$.)

(d)

$$\begin{aligned} \sum_{P \in \mathscr{P}} \left(2(1 - g(P)) - \sum_{E \in \partial P} n(E)/2 \right) \\ \leq -card(\mathscr{E}_{a11}) + \begin{cases} card\{V \in \mathscr{C}_{1l}: n(E'(V)) = 0\} & \text{if HZ holds,} \\ card\{V \in \mathscr{C}_2 \cup \mathscr{C}_3: n(E'(V)) = 0\} & \text{in general.} \end{cases} \end{aligned}$$

(*Recall that for* $V \in \mathscr{C}_2 \cup \mathscr{C}_3$, $E'(V)$ *is the edge in* $\mathscr{E}(B)$ *preceding the edge* $E \in \mathscr{E}(B)$ *for which* $V = V(E)$, *so that* $V(E_+(E'(V))) = V$.)

Proof. (a) This is obvious, since $n(E)$ is always 0, 1, or 2.

(b) From the definitions, we see that, for each E in ∂P,

$$\alpha(E) = -\pi + \gamma(E) + \pi n(E) + 2\pi\delta(E),$$

where $\delta(E) = 1$ if $E \in \mathscr{E}_3$ and is 0 otherwise. Summing over all E in ∂P and applying Proposition 2(a) gives the first inequality.

The second inequality is proved by considering the angles on the sphere at $v_0(P)$ between the images $v_1(E)$ of successive edges of ∂P and looking at how many times the sum of these angles wraps around $v_0(P)$; these angles are precisely the $\alpha(E)$ defined in Section 4 (and they are always nonnegative). A crucial fact is that the angles must wrap around exactly an integral number of times, since we begin and end with v_1 of the same edge.

Let $E_1, \ldots, E_n$ be a maximal sequence of edges labeled *regular* in ∂P. Note that by hypothesis H2, every $E \in \partial P$ such that $E \in \mathscr{E}_{a11} \cup \mathscr{E}_3$ lies in some such sequence. However, not all edges in ∂P can be in $\mathscr{E}_{a11} \cup \mathscr{E}_3$, since then, by H3, $v_1(E_i)$ would be in the same tie region for each i, all with $v_0(P)$ as an endpoint and going

counterclockwise around it; this is impossible, since we have to get back to $v_1(E_1)$ and $v_0(P)$ is on the boundary, not the interior, of the tie region. So suppose $E \in \mathscr{E}_{a11} \cup \mathscr{E}_3$ for $k = i, i+1, \ldots, j \leq n$ and $E_{j+1} \notin \mathscr{E}_{a11} \cup \mathscr{E}_3$; if all edges in ∂P are labeled *regular*, then number the edges so that $i = 1$. By hypothesis H3, $\bigcup_{k=i}^{j} v_2(V(E_k))$ lies in one tie region (and thus $i = j$ if that tie region is triangular). Furthermore, $Label(E_j) = regular = Label(E_{j+1})$, so $j + 1 \leq n$. Note that $\alpha(E_k)$ is 2π less the angle at $v_0(P)$ of a subregion of that tie region. Either $\alpha(E_{j+1})$ and the angles at subsequent negative-curvature corners (if any) within the maximal sequence sweep completely through that tie region and go on into another tie region, and thus have an α which is at least the sum of the differences of each of the previous angles from 2π, or the next edge in $\mathscr{E}_{a11} \cup \mathscr{E}_3$ in the maximal sequence has its image under v_1 lying within the same tie region. We see that if all edges were labeled *regular*, so that this maximal sequence encompassed all of ∂P, we would have

$$2\pi \, card\{E \in \partial P: E \in \mathscr{E}_{a11} \cup \mathscr{E}_3\} - \sum_{1}^{n} \alpha(E_j) \leq 0,$$

and hence

$$\sum_{E \in \partial P} (\pi - \gamma(E)) \leq 0,$$

which would contradict Proposition 2(a). (It is this step in the proof that invokes H3 and prevents occurrences of mesas as in Fig. 2(b).)

Thus we see that there is an edge E following E_n and it has $Label(E) = inverse$, so hypothesis H2 guarantees that $v_1(E)$ is a tie line of the n-diagram. Again we get

$$2\pi(j - i + 1) - \sum_{1}^{n} \alpha(E_j) \leq 0.$$

Since $\alpha(E) > 0$ for every E and in particular for those E with $Label(E) = inverse$ (and since $E \notin \mathscr{E}_{a11} \cup \mathscr{E}_3$ for those edges — it is this step which prevents the occurrence of steps as in Fig. 2(a)), we sum over all edges in δP to conclude

$$2\pi \, card\{E \in \partial P: E \in \mathscr{E}_{a11} \cup \mathscr{E}_3\} - \sum_{E \in \partial P} \alpha(E) < 0.$$

Since this quantity is an integral multiple of 2π, we obtain the second inequality.

(c) Since there is an edge in ∂P which is in $\mathscr{E}(B)$, there are corners V_1 and V_2 in $\mathscr{C}_2 \cup \mathscr{C}_3$ at the end and beginning respectively of some connected string of edges in both $\mathscr{E}(B)$ and ∂P; either there is one edge in $\mathscr{C}_0$ between E_2 and E_1 or there is one such edge followed by one or more pairs of alternating edges in $\mathscr{C}_1$ and $\mathscr{C}_0$. Let E_1 (resp. E_2) be the edge such that $V_1 = V(E_1)$ (resp. $V_2 = V(E_2)$); note that

$n(E_1) = 1 = n(E_2)$. Thus $\sum_{E \in \partial P} n(E)/2$ is at least 1; since it is even, it must be at least 2 unless for all other E in δP (and in particular, such E with $V(E) \in \mathscr{C}_0$), $n(E) = 0$; this is the second part of the conclusion of part (c). If we assume hypothesis HZ, then in this case where $\sum n(E)/2 = 1$ we will show that there must be a corner V in δP which is also in $\mathscr{C}_1$, which implies the HZ part of part (c).

We assume $\sum n(E)/2 = 1$ and thus that $n(E) = 0$ for all interior edges except E_2. If each such E is labeled *inverse*, then $\gamma(E) > \pi$ for each such E except the last (E_2), so

$$\pi - \gamma(E_1) + \sum_{E \in \partial P \cap \mathscr{E}(I)} (\pi - \gamma(E)) < 2\pi,$$

which would contradict Proposition 2(a) unless there were another E in ∂P with $\gamma(E) < \pi$; for such an E, $V(E) \in \mathscr{C}_1$.

If all interior edges are labeled *regular*, then as in the proof of part (b), the sum of the exterior angles $\gamma(E)$ of P over the interior edges E is less than π; hypothesis HZ plays the role of the second part of hypothesis H2 in forcing the final angle $\alpha(E_2)$ to finish sweeping out an entire tie region, and the fact that $n(E_2) = 1$ accounts for the π. Therefore (assuming that $n(E) = 0$ for all E except E_1 and E_2)

$$\begin{aligned} &\pi - \gamma(E_1) + \sum_{E \in \partial P \cap \mathscr{E}(I)} (\pi - \gamma(E)) \\ &\quad \leq \pi - \gamma(E_1) + \pi \\ &\quad < 2\pi. \end{aligned}$$

By Proposition 2(a), therefore, there must be at least one more E with $\gamma(E) < \pi$; for such an E, $V(E) \in \mathscr{C}_1$.

(d) Sum the results of parts (a), (b), and (c) and rearrange to get

$$\begin{aligned} (2(1 - g(P)) - \sum_{E \in \partial P} n(E)/2) \leq &-card\{E \in \partial P \cap \mathscr{E}_{a11}\} \\ &+ \begin{cases} card\{V \in \mathscr{C}_{1l} \cap \partial P : n(E'(V)) = 0\} & \text{if HZ holds,} \\ 1 - d & \text{in general,} \end{cases} \end{aligned}$$

and then sum over all P. □

Proposition 6. *Let T be the set of corners V in $\mathscr{C}_3$ such that*

(i) *equality holds in Proposition 2(c),*
(ii) *$n(E'(V)) = 1$ (recall that $E'(V)$ is the edge in $\mathscr{E}(B)$ preceding the edge E_1 in $\mathscr{E}(B)$ for which $V = V(E_1)$), and*
(iii) *$V_i(E'(V)) \notin \mathscr{C}_1$.*

Let $X = card\{V \in \mathscr{C}_{11}: n(E'(V)) = 0\}$ *if HZ holds, or* $card\{V \in \mathscr{C}_3 \cup \mathscr{C}_2: n(E'(V)) = 0\}$ *in general. Then*

$$\begin{aligned} &card(\mathscr{V}_3) + \sum_{V \in \mathscr{V}_{12}} m(V) + card(\mathscr{E}_{a11}) \\ &\quad \leq -2\chi(S) + X + (\tfrac{1}{2})\, card\{V \in \mathscr{C}_2: n(E'(V)) = 1\} \\ &\qquad -(\tfrac{1}{2})\, card(\mathscr{C}_3 \sim T) - M, \end{aligned}$$

where $0 \leq M = \sum_{V \in \mathscr{C} \sim \mathscr{V}_{12}} m(V)$.

Proof. We combine the results of Proposition 4 and 5(d) to get

$$\begin{aligned} &card(\mathscr{V}_3) + \sum_{V \in \mathscr{C}(I)} m(V) + 2\chi(S) + 2 \sum_{P \in \mathscr{P}} g(P) \\ &\quad -(\tfrac{1}{2})\, card\{V \in \mathscr{C}_0: n(E(V)) = 1\} \\ &\quad + card(\mathscr{C}_3) - (\tfrac{1}{2})\, card\left\{V \in \mathscr{C}_3: \sum_E (1 - n(E)/2) = \tfrac{3}{2}\right\} \\ &\leq \sum_{P \in \mathscr{P}} (2 - \sum_{E \in \partial P} n(E)/2) \\ &\leq X + 2 \sum_{\mathscr{P}} g(P) - card(\mathscr{E}_{a11}). \end{aligned}$$

This rearranges to

$$\begin{aligned} &card(\mathscr{V}_3) + (\tfrac{1}{2})\, card(\mathscr{C}_3) + \sum_{V \in \mathscr{V}_{12}} m(V) + card(\mathscr{E}_{a11}) \\ &\leq X - 2\chi(S) - \sum_{V \in \mathscr{C}(I) \sim \mathscr{V}_{12}} m(V) + (\tfrac{1}{2})\, card\{V \in \mathscr{C}_0: n(E(V)) = 1\} \\ &\quad -(\tfrac{1}{2})\, card(\mathscr{C}_3) + (\tfrac{1}{2})\, card\{V \in \mathscr{C}_3: \textstyle\sum (1 - n(E)/2) = \tfrac{3}{2}\}. \end{aligned}$$

We use the definition of T and the fact that if $n(E(V)) = 1$ for $V \in \mathscr{C}_0$, then the next corner which lies on the boundary B ($= V(E'(V))$) is in $\mathscr{C}_2 \cup \mathscr{C}_3$ to get

$$\begin{aligned} &card(\mathscr{V}_3) + (\tfrac{1}{2})\, card(\mathscr{C}_3) + \sum_{V \in \mathscr{V}_{12}} m(V) + card(\mathscr{E}_{a11}) \\ &\quad \leq X - 2\chi(S) - \sum_{V \in \mathscr{C}(I) \sim \mathscr{V}_{12}} m(V) \\ &\qquad + (\tfrac{1}{2})\, card\{V \in \mathscr{C}_2: n(E'(V)) = 1\} + (\tfrac{1}{2})\, card(T). \end{aligned}$$

□

Theorem 7. *Assume S is a two-dimensional locally embedded manifold in* R^3 *satisfying hypotheses S1 and* H1–H3 *and having plane segments, boundary line segments, etc., as defined in Sections* 1 *and* 4. *Then*

(1) *if hypothesis* HZ *holds, then the number of interior corners of* S *is less than*

$$(1 + A/a + \pi/a)(N_B - 2\chi(S))$$

and the number of plane segments in S *is less than*

$$(\tfrac{3}{2} + A/a + \pi/a)(N_B - 2\chi(S));$$

(2) *if* HZ *does not hold, these bounds are, respectively*

$$(1 + A/a + \pi/a)(N_B - 2\chi(S)) + (\tfrac{1}{2})(1 + A/a)\, card(\mathscr{C}_3)$$

and

$$(\tfrac{3}{2} + A/a + \pi/a)(N_B - 2\chi(S)) + (\tfrac{1}{2})N_B + (\tfrac{3}{2} + A/2a)\, card(\mathscr{C}_3).$$

(3) *More precisely, with* X *and* T *as defined in Proposition* 6, *and with* $N_+ = card(\mathscr{V}_3) + \sum_{V \in \mathscr{V}_{12}} m(V) + card(\mathscr{E}_{a11})$, *we have*

$$N_+ \leq -2\chi(S) + X + (\tfrac{1}{2})(card\{V \in \mathscr{C}_2 : n(E'(V)) = 1\} - card(\mathscr{C}_3 \sim T)),$$

$$card(\mathscr{C}(I)) \leq (1 + A/a)N_+ + (1/a)\left(-2\pi\chi(S) + \sum_{V \in \mathscr{C}(B)} (\kappa(V) + K(V))\right),$$

$$card(\mathscr{P}) \leq -\chi(S) + card(\mathscr{C}(I)) + (\tfrac{1}{2})\, card(\mathscr{C}_{1l}) + card(\mathscr{C}_2) + card(\mathscr{C}_3).$$

(4) *Equality holds in the bounds in* (3) *above on* N_+ *and* $card(\mathscr{C}(I))$ *when* $A = a$, *hypothesis* HZ *holds, and the surface* S *itself is in a kind of "general position" defined by the following properties: all interior corners are of type* 3 *or* 4, *equality holds in Proposition* 2(c) *for all boundary corners,* $g(P) = 0$ *for each plane segment* P, *and* $\sum_{E \in \partial P} n(E) = 4$ *for each plane segment* P *except those with a corner* V *in* $\mathscr{C}_{1l}$ *for which* $n(E'(V)) = 0$ *and for those the sum is* 2. (*Note that* $A = a$ *implies that only three faces meet at any vertex of* W *and hence* $card(\mathscr{V}_{12}) = card(\mathscr{E}_{a11}) = 0$.) *Equality holds in the more precise bound for* $card(\mathscr{P})$ *if the number of edges around each plane segment is four (which is in general not a reasonable expectation).*

Proof. The bound on N_+ was proved in Proposition 6. Using the fundamental facts on the quantization of Gauss curvature stated in Proposition 2(d), we see that

$$\begin{aligned} card(\mathscr{C}(I)) &= card(\mathscr{V}_3 \cup \mathscr{V}_{12} \cup \mathscr{V}_{a11}) \\ &\quad + card\{V \in \mathscr{C}(I) \sim (\mathscr{V}_3 \cup \mathscr{V}_{12} \cup \mathscr{V}_{a11})\} \\ &\leq card(\mathscr{V}_3 \cup \mathscr{V}_{12} \cup \mathscr{V}_{a11}) + \sum_{V \in \mathscr{C}(I) \sim (\mathscr{V}_3 \cup \mathscr{V}_{12} \cup \mathscr{V}_{a11})} - K(V)/a \\ &\leq (1 + A/a)N_+ + (1/a)\left(\sum_{V \in \mathscr{C}} - K(V) + \sum_{V \in \mathscr{C}(B)} K(V)\right). \end{aligned}$$

Applying Lemma 3 we obtain

$$card(\mathscr{C}(I)) \leq (1 + A/a)N_+ + (1/a)\left(-2\pi\chi(S) + \sum_{V \in \mathscr{C}(B)} \kappa(V) + \sum_{V \in \mathscr{C}(B)} K(V)\right),$$

which is the more precise estimate on $card(C(I))$ of the theorem. The statement concerning equality comes from noting the possible sources of inequality at each stage of the argument.

The simpler estimates of the theorem also follow directly from the above bound, using $\kappa(V) < \pi$ for each $V \in \mathscr{C}_2 \cup \mathscr{C}_1$ and $\kappa(V) = 0$ otherwise, $K(V) < 0$ for $V \in \mathscr{C}(B)$, $card(\mathscr{C}_1 \cup \mathscr{C}_2) = N_B$, and careful bookkeeping on corners in $\mathscr{C}_3$ in case HZ does not hold.

By the definition of the Euler characteristic,

$$card(\mathscr{P}) = \chi(S) + \sum_{\mathscr{P}} g(P) - card(\mathscr{C}(I)) - card(\mathscr{C}(B)) + (\tfrac{1}{2})(card(\mathscr{E}) + card(\mathscr{E}(B))).$$

Since there are at least four edges in $\mathscr{E}$ for each $P \in \mathscr{P}$ (by Proposition 5(b) and (c); remember the use of midpoints $\mathscr{C}_0$) and each (oriented) edge is in exactly one plane segment, we have that

$$4\, card(\mathscr{P}) \leq card(\mathscr{E})$$

or, more precisely,

$$4\, card(\mathscr{P}) \leq card(\mathscr{E}) - 2\, card(\mathscr{C}_1) + card(\mathscr{C}'_{1l}),$$

where $\mathscr{C}'_{1l}$ is the set of $V \in \mathscr{C}_{1l}$ such that $P(V)$ contains no interior corners.

We put this lower bound on $card(\mathscr{E})$ into the formula for $card(\mathscr{P})$ to obtain

$$card(\mathscr{P}) \geq \chi(S) + \sum_{\mathscr{P}} g(P) - card(\mathscr{C}(I)) - (\tfrac{1}{2})\, card(\mathscr{C}(B))$$

$$+ 2\, card(\mathscr{P}) + card(\mathscr{C}_1) - (\tfrac{1}{2})\, card(\mathscr{C}'_{1l}).$$

Note that $(\frac{1}{2})\, card(\mathscr{C}(B)) = card(\mathscr{C}_1 \cup \mathscr{C}_2 \cup \mathscr{C}_3)$. Thus when terms in $card(\mathscr{P})$ are combined and $\sum g(P)$ is dropped and this formula for $(\frac{1}{2})\, card(\mathscr{C}(B))$ is used, we get

$$card(\mathscr{P}) \leq -\chi(S) + card(\mathscr{C}(I)) + card(\mathscr{C}_2) + card(\mathscr{C}_3) + (\tfrac{1}{2})\, card(\mathscr{C}'_{1l}),$$

as claimed.

We get the simplified bound for $card(\mathscr{P})$ in the general case by replacing $card(\mathscr{C}(I))$ by its simplified bound. However, if we did that for the case when HZ holds, we would obtain a term involving $card(\mathscr{C}_3)$; we are trying to avoid such

terms when possible so that only N_B and $\chi(S)$ appear in the bound. Thus we apply the more precise bound for $card(\mathscr{C}(I))$ to get

$$\begin{aligned} card(\mathscr{P}) \leq (1 + A/a)(-2\chi(S) + X + (\tfrac{1}{2})(card\{V \in \mathscr{C}_2 : n(E'(V)) = 1\} \\ + card(T) - card(\mathscr{C}_3))) \\ + (1/a)(-2\pi\chi(S) + \sum_{V \in \mathscr{C}(B)} (\kappa(V) + K(V))) - \chi(S) \\ + card(\mathscr{C}_2) + card(\mathscr{C}_3) + (\tfrac{1}{2})\, card(\mathscr{C}'_{1l}). \end{aligned}$$

We would like

$$card(\mathscr{C}_3) + (1 + A/a)(\tfrac{1}{2})(card(T) - card(C_3)) - \sum_{V \in \mathscr{C}_3} - K(V)/a$$

to be nonpositive so that all these terms can be dropped; we note that it is bounded above by

$$card(\mathscr{C}_3) + (1 + A/a)(\tfrac{1}{2})(card(T) - card(\mathscr{C}_3)) - card\{V \in \mathscr{C}_3 : K(V) \leq -a\}.$$

As stated in Proposition 2(*d*), under hypothesis HZ, $K(V) \geq -a$ for all $V \in T$, so the above is less than or equal to

$$\begin{aligned} card\{V \in \mathscr{C}_3 : K(V) > -a\} + (1 + A/a)(\tfrac{1}{2})(-card\{V \in \mathscr{C}_3 : K(V) > -a\}) \\ -(1 + A/a)(card(\mathscr{C}_3) - card(T)), \end{aligned}$$

which is indeed nonpositive since $(1 + A/a)(\tfrac{1}{2}) \geq 1$ and T is contained in $\mathscr{C}_3$. Thus with hypothesis HZ, we have

$$\begin{aligned} card(\mathscr{P}) &\leq -\chi(S) + card(\mathscr{C}_2) + (1 + A/a)(-2\chi(S) + card(\mathscr{C}_{1l}) + (\tfrac{1}{2})\, card(\mathscr{C}_2)) \\ &\quad + (1/a)\left(-2\pi\chi(S) + \sum_{V \in \mathscr{C}_1 \cup \mathscr{C}_2} (\kappa(V) + K(V))\right) + (\tfrac{1}{2})\, card(\mathscr{C}'_{1l}) \\ &< -\chi(S) + (1 + A/a)(-2\chi(S) + card(\mathscr{C}_2 \cup \mathscr{C}_1)) \\ &\quad + (\pi/a)(-2\chi(S) + N_B) + (\tfrac{1}{2})\, card(\mathscr{C}'_{1l}) \\ &= -\chi(S) + (1 + A/a + \pi/a)(-2\chi(S) + N_B) + (\tfrac{1}{2})\, card(\mathscr{C}'_{1l}) \\ &\leq (\tfrac{3}{2} + A/a + \pi/a)(-2\chi(S) + N_B), \end{aligned}$$

as claimed. □

Note. The appearance of $card(\mathscr{C}_3)$ in the non-HZ-case bound means that we have to know enough about the structure of S along B to know how many corners

there are in the middle of boundary line segments. If we think of extracting S from a larger surface by drawing a boundary B on that larger surface, then for the generic choice of such a B, $card(\mathscr{C}_3)$ will be zero, as in hypothesis HB in Section 1.

6. Examples

We present six examples of surfaces with boundary which satisfy hypotheses S1 and H1–H3, comparing the actual number of interior corners and plane segments to the bounds of Theorem 7. We also use these examples and their corresponding figures to demonstrate some of the definitions of Section 4.

For each of these examples, we use any surface energy function Φ whose Wulff shape W is such that its n-diagram is as shown (in stereographic projection) in Fig. 1(a). For example, W could be a 14-sided figure obtained by cutting off squarely the corners of a regular octahedron as shown in Fig. 1(b); each square face could have a different size and still the n-diagram would be the given one. Any W with this n-diagram is a generalised zonahedron since the union of the tie lines of the n-diagram is a set of complete great circles. Note that $a = A = \pi/6$ for this n-diagram. The vertices of the n-diagram and the directions perpendicular to the great circles of its tie lines are given in Table 1. A physical example of such a Φ is that for a potassium aluminum alum crystal in a saturated solution [B2].

In each example, we let the set of boundary line segments be $\{B_i, i = 1, \ldots, N_B\}$, with the index i increasing in positive direction of the boundary, and we let V_i be the final corner of the line segment B_i for each $i = 1, \ldots, N_B$.

Table 1. Names for directions of edges and faces of the W used in the examples.

Faces	n1	n2	n3	n4
	$(1, 0, 0)$	$(0, 1, 0)$	$(0, 0, 1)$	$\left(\frac{1}{\sqrt{3}}, \frac{1}{\sqrt{3}}, \frac{1}{\sqrt{3}}\right)$
	n8 = −n7	n9 = −n6	n10 = −n5	n11 = −n4
Edges	A	B	C	D
	$\left(\frac{1}{\sqrt{2}}, -\frac{1}{\sqrt{2}}, 0\right)$	$\left(\frac{1}{\sqrt{2}}, \frac{1}{\sqrt{2}}, 0\right)$	$\left(0, \frac{1}{\sqrt{2}}, -\frac{1}{\sqrt{2}}\right)$	$\left(\frac{1}{\sqrt{2}}, 0, -\frac{1}{\sqrt{2}}\right)$
Faces	n5	n6	n7	
	$\left(\frac{1}{\sqrt{3}}, \frac{1}{\sqrt{3}}, -\frac{1}{\sqrt{3}}\right)$	$\left(-\frac{1}{\sqrt{3}}, \frac{1}{\sqrt{3}}, -\frac{1}{\sqrt{3}}\right)$	$\left(-\frac{1}{\sqrt{3}}, \frac{1}{\sqrt{3}}, \frac{1}{\sqrt{3}}\right)$	
	n12 = −n3	n13 = −n2	n14 = −n1	
Edges	E	F		
	$\left(\frac{1}{\sqrt{2}}, 0, \frac{1}{\sqrt{2}}\right)$	$\left(0, \frac{1}{\sqrt{2}}, \frac{1}{\sqrt{2}}\right)$		

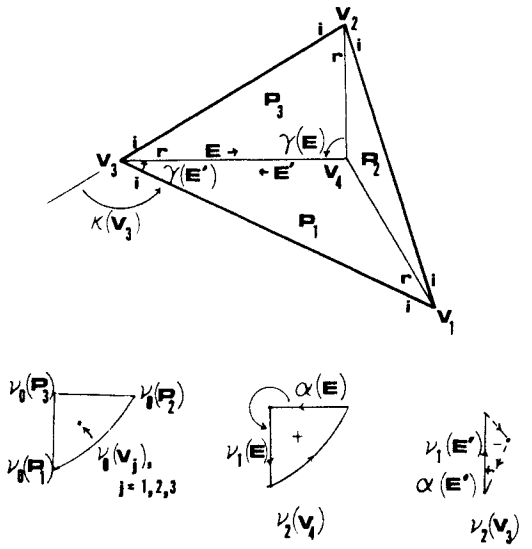

Fig. 7. The surface of Example 1, together with some of its associated Gauss maps and angles. *Regular* edges are labeled **r** and *inverse* edges are labeled **i**.

Example 1 (see Fig. 7). Here B consists of three line segments; HZ does not hold since these line segments are not parallel to edges of W. Thus Theorem 7 gives no bound on the number of interior corners or plane segments depending only on N_B and $\chi(S)$; we need to look at S near B enough to see that $card(\mathscr{C}_3) = 0$ (there are no corners of S in the middle of line segments of B) to obtain the bounds $card(\mathscr{C}(I)) < (1 + 1 + 6)(3 - 2) = 8$ and $card(\mathscr{P}) < (\frac{3}{2} + 1 + 6)(3 - 2) + \frac{3}{2} = 10$. We expect these bounds to be much too large since the Gauss curvature of S at the boundary corners was ignored and the curvature κ of B at each of those corners was replaced by π in deriving these bounds.

In fact, S consists of three plane segments and these plane segments meet in precisely one interior corner V_0, which is a convex type-3 corner; the more precise bounds of the theorem should yield exactly these numbers, since $a = A$ and we see that S is in the type of general position specified in the theorem and that there are exactly four edges in $\mathscr{E}$ for each plane segment (remember that we insert midpoint corners into geometric edges of S along B). We compute these more precise bounds using only information about S near B (and $\chi(S) = 1$) as follows. For $i = 1, 2, 3$, $\nu_2(V_i)$ is a subset, negatively oriented, of the tie region whose vertices are the directions of the three plane segments; these subsets are disjoint except along their boundaries and their union is the whole tie triangle. Thus $a = -K(V_1) - K(V_2) - K(V_3)$. We note that the interior edges which have a corner in $\mathscr{C}(B)$ as initial or final corner (this includes all interior edges in this example) are of *regular* type; thus all boundary edges are labeled *inverse* by the convention of Section 4, in order that the label will change at each wedge with one interior and one boundary edge. We see that this means all edges from a corner of B to a boundary midpoint corner have $n = 0$. $\kappa(V_1) + \kappa(V_2) + \kappa(V_3) = 2\pi$, since the three corners are coplanar. We

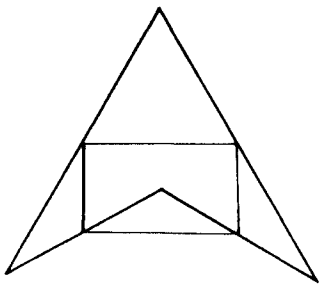

Fig. 8. The surface of Example 2.

therefore obtain

$$card\{V\colon K(V) > 0\} \leq -2\chi(S) + X + (\tfrac{1}{2})\, card\{V \in \mathscr{C}_2\colon n(E'(V)) = 1\} = 1,$$

since $X = card\{V \in \mathscr{C}_2\colon n(E'(V)) = 0\} = 3$. The more precise bound on $card(\mathscr{C}(I))$ $(1 \leq (1+1)(1) + 6(-2 + 2 - \frac{1}{6}))$ is also an equality, as claimed. The more precise bound on $card(P)$ is then $-1 + 1 + 3$ and is also exact.

Example 2 (see Fig. 8). Here B is a skew quadrilateral; since its line segments are parallel to edges of W, HZ holds and we know immediately (using $\chi(S) = 1$) that $card(\mathscr{C}(I)) < (1 + 1 + 6)(4 - 2) = 16$ and $card(\mathscr{P}) < (\frac{3}{2} + 1 + 6)(4 - 2) = 17$. Again, we expect these bounds to be much too large because we overestimated many quantities to get these bounds. S in fact has no interior corners and consists of five plane segments, one spanning each corner of B and one hanging in the middle with a corner on each boundary line segment. We will compute the more precise bounds using only information on S near B; knowing this local structure of S near B we can tell that they will in fact be exact since S is in the kind of general position specified by the theorem and since there are just the minimum number of edges around each plane segment.

We note $card(\mathscr{C}_2) = 0$, $card(\mathscr{C}_3) = 4$, and $card(\mathscr{C}_1) = card(\mathscr{C}_{1l}) = 4$. For each $i = 1, 2, 3, 4$, $\kappa(V_i) = 2\pi/3$ and $K(V_i) = 0$. For each $V \in \mathscr{C}_3$, $\kappa(V) = 0$ and $K(V) = -a$. Since edges around the hanging plane have their labels alternating, the convention that $n(E) = 1$ when the wedge of E contains one interior and one boundary edge (and that the label changes on a string of boundary edges only when it is forced to) turns out to require that all the boundary edges between any successive pair of corners in $\mathscr{C}_3$ have the same label. Thus the bound on $card\{V\colon K(V) > 0\}$ is $-2 + 4 + (\frac{1}{2})(0 - 4) = 0$ (whether we use the formula for X appropriate to HZ or not) and the more precise bound on $card(\mathscr{C}(I))$ is $(1 + 1)(0) + 6(-2 + 4(\frac{2}{3}) - 4(\frac{1}{6})) = 0$, as claimed. The more precise bound on $card(\mathscr{P})$ is $-1 + 0 + 2 + 4 = 5$, which is indeed exact.

Example 3 (see Fig. 9). Here B consists of eight line segments forming one simple closed curve; each of these line segments is parallel to an edge of W so HZ holds. We immediately conclude (using $\chi(S) = 1$) that $card(\mathscr{C}_i) < (1 + 1 + 6)(8 - 2) = 48$ and $card(\mathscr{P}) < (\frac{3}{2} + 1 + 6)(8 - 2) = 51$, but expect these bounds to be much too

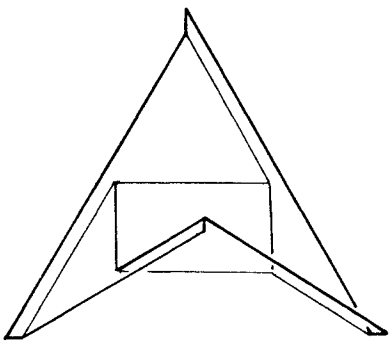

Fig. 9. The surface of Example 3.

large. In fact, S again has five plane segments; the S of the previous example is a subsurface of this S, but the four outer plane segments have been extended so that there are now four interior type-4 corners and $\mathscr{C}_3$ is empty. Half of the corners of B are in $\mathscr{C}_{1l}$ and for them $\kappa = 2\pi/3$; the other half are in $\mathscr{C}_2$ and for them $\kappa = \pi/3$ and $K = -2a = -\pi/3$. The labels on boundary edges turn out to have to change just before each $V \in \mathscr{C}_2$. The bound on $card\{V\colon K(V) > 0\}$ is exact whichever definition of X is used: $-2 + 0 + (\frac{1}{2})(4 - 0) = 0$. The more precise bound on $card(\mathscr{C}(I))$ is also exact $((1 + 1)(0) + (6)(-2 + 4(\frac{2}{3}) + 4(\frac{1}{3} - \frac{1}{3})) = 4)$ but the more precise bound on $card(\mathscr{P})$ $((-1 + 4 + (\frac{1}{2})4 + 4 = 9))$ is off because there is one more edge on each of the outer plane segments than the minimum which went into computing the bound.

Example 4 (see Fig. 10). Here B consists of 16 line segments; HZ holds, and $\chi(S) = 1$. Thus we know that $card(\mathscr{C}(I)) < (1 + 1 + 6)(16 - 2) = 112$ and

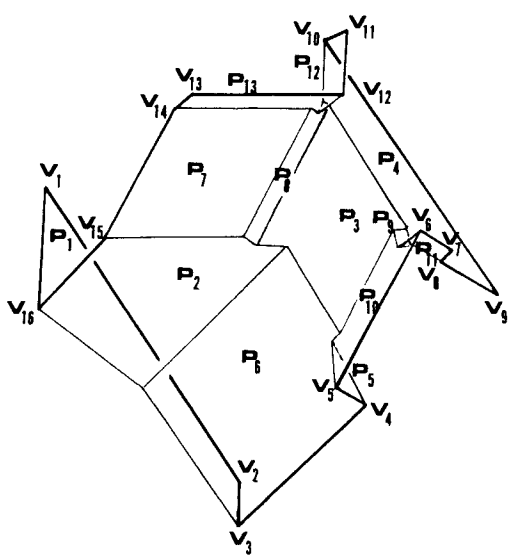

Fig. 10. The surface of Example 4; see also Tables 1 and 2.

$card(\mathscr{P}) < (\frac{3}{2} + 1 + 6)(16 - 2) = 119$, but we expect these bounds to be much too large.

Looking at S near B, we see that six of the boundary corners are in $\mathscr{C}_1$ and the other ten are in $\mathscr{C}_2$; the values of $\kappa(V_i)$, $K(V_i)$, and, where appropriate, $n(E'(V_i))$ are given in Table 2. Thus the more precise bounds are

$$\begin{aligned} card(\mathscr{C}_+) &\leq -2 + 2 + (\tfrac{1}{2})(6) - 0 = 3, \\ card(\mathscr{C}(I)) &\leq (1 + 1)(3) + 6(-2 + \tfrac{20}{3} - \tfrac{16}{6}) = 18, \\ card(\mathscr{P}) &\leq -1 + 18 + (\tfrac{1}{2})(5) + 10 + 0 = 29\tfrac{1}{2}. \end{aligned}$$

In fact, S has one positive-curvature corner (where P_2, P_7, P_8 intersect), 14 interior corners, and 13 plane segments. The bounds on $\mathscr{C}_+$ and $\mathscr{C}(I)$ fail to be exact because the bounds of Proposition 5 are not exact for P_k with $k = 2, 4, 6, 10$.

Example 5 (see Fig. 11). The surface has the same boundary B as the previous surface and the same Euler characteristic; therefore the bounds which do not require knowing anything else about S are the same. However, this surface is different near B compared with the previous surface; the new values of K and n are given in Table 3 (the values of κ remain the same since they depend only on B). There are also eight new corners in $\mathscr{C}(B)$, all in $\mathscr{C}_3$, and the information on them is also in Table 3. The more precise bounds are now

$$\begin{aligned} card(\mathscr{C}_+) &\leq -2 + 7 + (\tfrac{1}{2})(2) - (\tfrac{1}{2})(6) = 3, \\ card(\mathscr{C}(I)) &\leq (1 + 1)(3) + 6(-2 + \tfrac{20}{3} - \tfrac{18}{6}) = 16, \\ card(\mathscr{P}) &\leq -1 + 16 + (\tfrac{1}{2})(9) + 4 + 8 = 31\tfrac{1}{2}. \end{aligned}$$

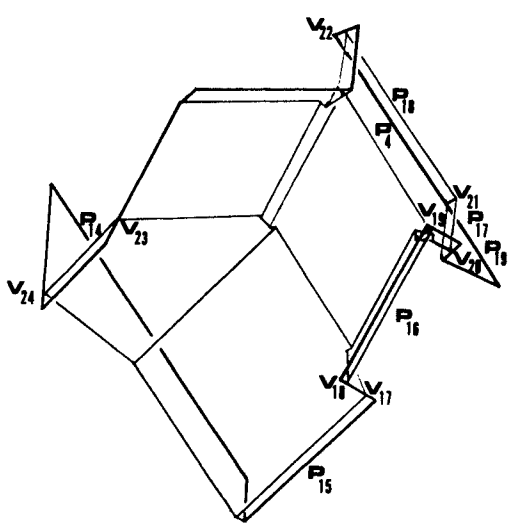

Fig. 11. The surface of Example 5; see also Tables 1–3.

Table 2. Information for Example 4.

i	1	2	3	4	5	6	7	8	9	10	11	12	13	14	15	16
$v(V_i)$	−B	−C	B	F	E	D	−E	−F	−E	C	F	B	A	−F	−D	−F
$\frac{\kappa(V_i)}{\pi}$	$\frac{2}{3}$	$\frac{1}{3}$	$\frac{1}{3}$	$\frac{1}{3}$	$\frac{1}{2}$	$\frac{1}{2}$	$\frac{1}{3}$	$\frac{1}{3}$	$\frac{2}{3}$	$\frac{1}{2}$	$\frac{1}{3}$	$\frac{1}{2}$	$\frac{1}{3}$	$\frac{1}{3}$	$\frac{1}{3}$	$\frac{1}{3}$
$\frac{K(V_i)}{\pi/6}$	0	0	−2	−1	−1	−1	0	−4	0	−1	0	−1	0	−2	−1	−2
$V_i \in$	$\mathscr{C}_1$	$\mathscr{C}_{1l}$	$\mathscr{C}_2$	$\mathscr{C}_2$	$\mathscr{C}_2$	$\mathscr{C}_2$	$\mathscr{C}_{1l}$	$\mathscr{C}_2$	$\mathscr{C}_{1l}$	$\mathscr{C}_2$	$\mathscr{C}_{1l}$	$\mathscr{C}_2$	$\mathscr{C}_{1l}$	$\mathscr{C}_2$	$\mathscr{C}_2$	$\mathscr{C}_2$
$n(E')$	—	0	0	1	1	0	1	1	0	0	1	1	1	1	1	0
k	1	2	3	4	5	6	7	8	9	10	11	12	13			
$v_0(P_k)$	n8	n5	n4	n7	n8	n1	n4	n2	n3	n9	n10	n6	n5			

Table 3. Additional information for Example 5.

i	1	2	3	4	17	18	5	6	19	7	20	8	9	21
$\frac{K(V_i)}{\pi/6}$	0	0	−2	0	−1	−1	0	0	−1	0	−2	−2	0	−1
$V_i \in$	$\mathscr{C}_1$	$\mathscr{C}_{1l}$	$\mathscr{C}_2$	$\mathscr{C}_{1l}$	$\mathscr{C}_3$	$\mathscr{C}_3$	$\mathscr{C}_1$	$\mathscr{C}_{1l}$	$\mathscr{C}_3$	$\mathscr{C}_{1l}$	$\mathscr{C}_3$	$\mathscr{C}_2$	$\mathscr{C}_{1l}$	$\mathscr{C}_3$
$n(E')$	—	0	0	0	0	1	—	0	0	1	1	1	0	0
i	10	22	11	12	13	14	23	15	16	24				
$\frac{K(V_i)}{\pi/6}$	0	−1	0	−1	0	−2	−2	0	0	−2				
$V_i \in$	$\mathscr{C}_{1l}$	$\mathscr{C}_3$	$\mathscr{C}_{1l}$	$\mathscr{C}_2$	$\mathscr{C}_{1l}$	$\mathscr{C}_2$	$\mathscr{C}_3$	$\mathscr{C}_1$	$\mathscr{C}_{1l}$	$\mathscr{C}_3$				
$n(E')$	0	0	0	0	1	1	1	—	0	0				
k	14	15	16	17	18	19								
$v_0(P_k)$	n6	n5	n13	n6	n14	n7								

The surface is obtained from the surface of Example 4 by changing the position of the four plane segments for which the estimates were previously not exact; in doing so, one of the plane segments (P_4) had to be split into two plane segments (P_4, P_{19}) and two plane segments (P_{17}, P_{18}) had to be added to accomplish that splitting; three more plane segments (P_{14}, P_{15}, P_{16}) had to be added along the boundary when the remaining three plane segments (P_2, P_6, P_{10} resp.) were moved. There are two new interior corners, both with $K > 0$ (one where P_1, P_6, P_{15} meet and one where P_4, P_{17}, P_{18} meet). As the surface is now in the type of "general position" specified in the theorem, the bound for the number of positive-curvature corners and the more precise bound on the total number of interior corners are exact.

Example 6 (see Fig. 12). Here there are 54 boundary components, each consisting

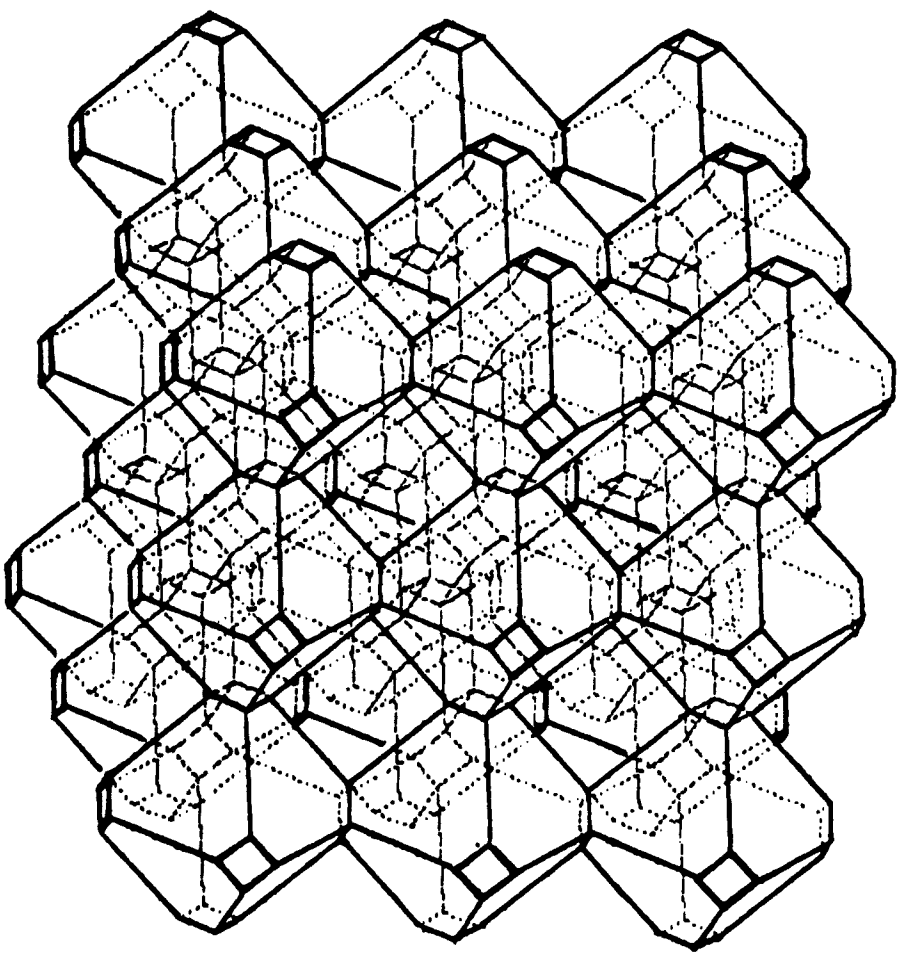

Fig. 12. The surface of Example 6, having 28 handles and 54 connected boundary components.

of four line segments, and

$$\chi(S) = 2 - 2 \times (\text{number of handles}) - (\text{number of boundary components})$$
$$= 2 - 56 - 54 = -108.$$

The boundary line segments are parallel to edges of W, so HZ is satisfied. We thus obtain

$$card(\mathscr{C}_i) < (1 + 1 + 6)(54(4) - 2(-108))$$

and

$$card(\mathscr{P}) < (\tfrac{3}{2} + 1 + 6)(54(4) - 2(-108));$$

these bounds are huge but certainly finite.

We now look at S near B in order to compute the more precise bounds. Each boundary corner is in $\mathscr{C}_2$ and has $\kappa(V) = \pi/2$ and $K(V) = -5a$. All boundary edges are labeled *inverse*. We thus have

$$card(\mathscr{C}_+) \leq -2(-108) + 0 + (\tfrac{1}{2})0 - 0 = 216,$$
$$card(\mathscr{C}(I)) \leq (1 + 1)(216) + 6((-2)(-108) + 4(54)(\tfrac{1}{2} - \tfrac{5}{6})) = 1296,$$

and

$$card(\mathscr{P}) \leq (-2)(-108) + 1296 + 54 = 1566.$$

In fact, S is constructed by taking 27 copies of the 2-skeleton of a centrally symmetric truncated octahedron with the same n-diagram as W, cutting out all their square faces, and then stacking them square boundary to square boundary, three deep in each coordinate direction. There are $4(54) = 216$ interior corners, each one satisfying H1 since it is a type-9 corner; there are $8(27) = 216$ plane segments in S. The more precise bounds of the theorem are not very good for two reasons: the interior corners have Gauss curvature $-4a$ rather than $-a$, and none of the allowed corners of positive Gauss curvature are present due to the positioning of the planes. With a slightly different positioning of the boundary components and plane segments, B should bound a surface with the same number of handles, with all 216 possible positive-curvature corners, and with each type-9 corner broken up into four type-4 corners; the more precise bound on $card(\mathscr{C}(I))$ would then be achieved.

References

[ATZ] J. E. Avron, J. E. Taylor, and R. K. P. Zia, Equilibrium shapes of crystals in a gravitational field: crystals on a table, *J. Statist. Phys.* **33** (1983), 493–522.

[B1] H. Busemann, The isoperimetric problem for Minkowski area, *Amer. J. Math.* **71** (1949), 743–762.

[B2] H. E. Buckley, *Crystal Growth*, Wiley, New York (1951), pp. 442 and 534.

[C1] H. S. M. Coxeter, The classification of zonohedra by means of projective diagrams, *J. Math. Pures Appl.* **41** (1962), 137–156, reprinted with improvements in *Twelve Geometric Essays*, Southern Illinois University Press, Carbondale, IL. (1968).

[C2] H. S. M. Coxeter, *Regular Polytopes*, Dover, New York (1973), pp. 28–31.

[F] E. S. Fedorov, Elemente der Gestaltenlehre, as abstracted in *Z. Kryst. Mineral.* **21** (1893), 679–694 (the definition of a zonohedron is on p. 688). The author is indebted to M. Senechal for verification of Fedorov's definition in the original Russian in *Nachala Ucheniya o Figurath, Notices of the Imperial Petersburg Mineralogical Society*, 2nd series, **24** (1885). 1–279 and reprinted in 1953 in the Soviet series "Classics of Science". See also the extended review of Fedorov's work by M. Senechal and R. Galiulin, An introduction to the study of figures: the geometry of E. S. Fedorov, *Structural Topology* **10** (1984), 5–22 (although that review uses Coxeter's definition).

[T1] J. E. Taylor, Crystalline variational problems, *Bull. Amer. Math. Soc.* **84** (1978), 569–588.

[T2] J. E. Taylor, Complete catalog of minimizing embedded crystalline cones, *Proc. Sympos. Pure Math.* **44** (1986), 379–403.

[T3] J. E. Taylor, Zonohedra and Generalized Zonohedra, *Amer. Math. Monthly* (to appear).

[T4] J. E. Taylor, Constructing crystalline minimal surfaces, in *Seminar on Minimal Submanifolds*, F. Bombieri, ed., Annals of Mathematics Studies, Vol. 105, Princeton University Press, Princeton, NJ (1983), pp. 271–288.

[T5] J. E. Taylor, Is there gravity-induced facetting in crystals?, *Astérisque* **118** (1984), 243–255.

[TC] J. E. Taylor and J. W. Cahn, Catalog of saddle-shaped surfaces in crystals, *Acta Metal.* **34** (1986), 1–12.

[VCMS] P. W. Voorhees, S. R. Coriell, G. B. McFadden, and R. F. Sekerka, The effect of anisotropic crystal-melt surface tension on grain-boundary groove morphology, *J. Cryst. Growth* **67** (1984), 425–440.

Received November 18, 1986, and in revised form January 2, 1990.